



1 **Planktic foraminifera assemblage composition and flux dynamics inferred from an annual**
2 **sediment trap record in the Central Mediterranean Sea**

3

4 Thibault M. Béjard^{1*}, Andrés S. Rigual-Hernández¹, Javier Pérez Tarruella¹, José-Abel Flores¹, Anna
5 Sanchez Vidal², Irene Llamas Cano², Francisco J. Sierro¹

6

7 1. Área de Paleontología, Departamento de Geología, Universidad de Salamanca, Salamanca, Spain

8 2. GRC Geociències Marines, Departament de Dinàmica de la Terra i de l'Oceà, Universitat de
9 Barcelona, Spain

10

11 * **Correspondence:** Thibault M. Béjard (thibault.bejard@usal.es)

12

13 **Keywords:** sediment trap - Sicily Strait - Mediterranean Sea - planktic foraminifera - seasonal
14 variations - environmental change

15

16 **Abstract**

17

18 The Sicily Strait, located in the Central Mediterranean Sea, represents a key point for the regional
19 oceanographic circulation as it is considered the sill that separates the western and eastern basins.

20 Therefore, it is considered a unique zone regarding the well-documented west-to-east
21 Mediterranean productivity gradient. Here we document the planktic foraminifera assemblages
22 retrieved by the C01 sediment trap between November 2013 and October 2014. 19 samples from
23 the sediment trap deployed at a water depth of around 400 m have been used. More than 3700
24 individuals and 15 different species have been identified. *Globorotalia inflata*, *Globorotalia*
25 *truncatulinoidea*, *Globigerina bulloides*, *Globigerinoides ruber* and *ruber* (pink) were the five main
26 species identified, accounting for more than 85% of the total foraminifera.

27 The total planktic foraminifera flux mean value was 630 shells m⁻² d⁻¹, with a minimum value of 45
28 shells m⁻² d⁻¹ displayed during late autumn 2013 and a maximum of 1890 shells m⁻² d⁻¹ reached
29 during spring 2014. Most of the species fluxes followed a similar pattern. This is likely the result of
30 the regional oceanographic configuration and the marked seasonality in the surface circulation.
31 During spring and winter, the Atlantic waters dominate the surface circulation, bringing cool and
32 nutrient enriched waters. This results in a planktic foraminifera flux increase and a dominance of
33 western basin taxa. During summer and autumn, the circulation is dominated by the eastern warm
34 and oligotrophic Levantine water, which results in planktic foraminifera flux decrease and the
35 dominance of eastern basin species. Our comparison with satellite derived SST and chlorophyll-*a* data
36 showed that *G. inflata* was associated with cool and nutrient rich conditions, while both *G. ruber*
37 morphotypes were associated with warm and oligotrophic conditions. However, no trends were
38 identified for *G. truncatulinoidea* or *G. bulloides*.

39 In addition, a comparison of the Sicily Strait data with other Mediterranean time series located in
40 the Alboran Sea, Gulf of Lions and the Levantine basin was carried out. Our data indicated that the
41 annualized planktic foraminifera flux was lower than in the westernmost Alboran Sea but higher
42 than in the easternmost Levantine basin. However, the Sicily Strait species diversity was the highest



43 among the compared zones, highlighting the influence of the different basins and its transitional
44 aspect from a planktic foraminifera population perspective.
45 Finally, we compared the sediment trap planktic foraminifera assemblage with the assemblages
46 from seabed sediment located in the vicinity of the Sicily Strait. Our results showed that the
47 sediment trap population significantly differed from the assemblages in the seabed sediment. The
48 deep-dwelling species dominated the sediment trap samples, while eutrophic and oligotrophic
49 species were significantly more abundant in the core-tops, highlighting a potential effect of the
50 recent Mediterranean environmental change, such as warming and a potential shift in the
51 oceanographical conditions on the planktic foraminifera population.

52

53 **1. Introduction**

54

55 Planktic foraminifera are a group of marine calcareous single-celled protozoans with a cosmopolitan
56 distribution. Around 50 morphospecies of planktic foraminifera have been described in today's
57 oceans (Schiebel and Hemleben, 2017), and although most of those species are surface dwellers,
58 some species can be found in waters below 2000 m (Schiebel and Hemleben, 2005). Their
59 abundance and distribution are affected by a wide array of factors, such as temperature, salinity,
60 chlorophyll-*a* and nutrient concentrations, among others (Hemleben et al., 1989; Schiebel and
61 Hemleben, 2005). According to Schiebel, (2002), the production and export of their calcareous shells
62 account for 23 to 56% of the open marine CaCO₃ flux, thereby playing a key role in the marine carbon
63 cycle. Moreover, the high preservation potential of their shells makes them one of the most used
64 groups for multi-proxy studies. Numerous paleoclimatic (e.g. Barker and Elderfield, 2002; Lirer et
65 al., 2014; Margaritelli et al., 2020; Sierro et al., 2005) and paleoceanographic (Cisneros et al., 2016;
66 Ducassou et al., 2018; Margaritelli et al., 2022; Toucanne et al., 2007) reconstructions have used
67 planktic foraminifera as a proxy. In addition, their capacity to reflect the water column's chemical
68 properties has propelled studies that have focused on the impact of recent climate and
69 environmental variability on the water column in different parts of the ocean (e.g. Azibeiro et al.,
70 2023; Beer et al., 2010; Bijma et al., 2002; Chapman, 2010; Marshall et al., 2013; Osborne et al.,
71 2016). As marine calcifying organisms, they are considered particularly vulnerable to the ongoing
72 ocean warming and acidification (Bijma et al., 2002; Fox et al., 2020). Shell calcification of several
73 foraminifera species has been showed to decrease in response to ocean acidification, and therefore,
74 changes in the weight of their shells are considered an indicator of the ocean acidification impact
75 on different timescales (Béjard et al., 2023; de Moel et al., 2009; Fox et al., 2020; Kroeker et al.,
76 2013; Moy et al., 2009; Pallacks et al., 2023). In contrast, ocean warming has been proposed to
77 produce an opposite effect on foraminifera calcification, as some studies have documented that an
78 increase in water temperature results in larger shells and enhanced growth rates (Lombard et al.,
79 2011, 2009; Schmidt et al., 2006).

80 Despite the wide array of studies focused on planktic foraminifera ecology and distribution, several
81 aspects of their ecology remain uncertain, such as their ecological tolerance limits (Mallo et al.,
82 2017), their geographical and temporal distributions and contribution to the marine biogeochemical
83 cycles (Jonkers and Kučera, 2015). As major contributors to the pelagic calcite production (Schiebel,
84 2002), understanding their life cycle on different time scales is essential for understanding the role



85 they play in the marine carbon cycle and the impact of environmental change on these organisms.
86 In this regard, sediment traps represent a powerful tool to improve our knowledge of planktic
87 foraminifera ecology and their impact on the biogeochemical cycles, as they allow the monitoring
88 of foraminifera shell fluxes for extended periods, thereby allowing to document their seasonal and
89 interannual variability and estimate their contribution to annual budgets of carbonate export to the
90 seafloor (Jonkers et al., 2019).
91 The Mediterranean Sea is a semi-enclosed sea often considered a “miniature ocean” (Bethoux et
92 al., 1999) from an oceanographic point of view or a “laboratory basin” (Bergamasco and Malanotte-
93 Rizzoli, 2010) for studying processes occurring on a global scale. In addition, it is supersaturated
94 regarding calcite (Álvarez et al., 2014), a key aspect in foraminifera studies, as this parameter favors
95 shell preservation and represents one of the main environmental controls on planktic foraminifera
96 abundance and calcification (Aldridge et al., 2012; Marshall et al., 2013; Osborne et al., 2016). These
97 features make it an interesting zone of the global ocean to study the life cycle and seasonal response
98 to changing environmental conditions of calcifying plankton. The Sicily Strait, in the central
99 Mediterranean, is the sill that divides the Mediterranean into its western and eastern basins. It is a
100 choke point for the regional surface and deep-water circulation (Malanotte-Rizzoli et al., 2014) and
101 a transition region regarding the well-known west-to-east oligotrophy gradient, functioning as a
102 “biological corridor” (Siokou-Frangou et al., 2010) known in the Mediterranean (Navarro et al.,
103 2017).
104 Despite these characteristics, time series that focused on planktic foraminifera in the Mediterranean
105 Sea are scarce. So far, the best monitored regions are the Alboran Sea (Bárcena et al., 2004;
106 Hernández-Almeida et al., 2011), the Gulf of Lions (Rigual-Hernández et al., 2012), and more
107 recently, the Levantine Basin (Avnaim-Katav et al., 2020). The latter studies showed that planktic
108 foraminifera followed a unimodal distribution with maximum shell export occurring during the
109 months of April-May, February-March and February respectively, which agreed with the local
110 hydrographic conditions. However, the central Mediterranean remains understudied and poorly
111 documented regarding both continuous time series and planktic foraminifera dynamics.
112 Therefore, this work aims to provide new planktic foraminifera data from a sediment trap mooring
113 line located in the Strait of Sicily to improve the current knowledge about their community
114 composition and seasonal patterns in the central Mediterranean. For that purpose, here we
115 document the magnitude and composition of planktic foraminifera fluxes identified in the >150 µm
116 fraction (i.e. the most commonly used size fraction for studying planktic foraminifera distribution)
117 from November 2013 to October 2014. We compare our planktic foraminifera data with a suite of
118 environmental parameters to assess the main environmental drivers that control the seasonal
119 variations in the composition and abundance of the sinking planktic foraminifera assemblages.
120 Lastly, to provide further insight on a regional and global scale of the planktic foraminifera
121 association and fluxes identified here, we compare our data with other time series from the
122 Mediterranean, Atlantic Ocean and other regions of the world’s oceans.



123 2. Study area

124

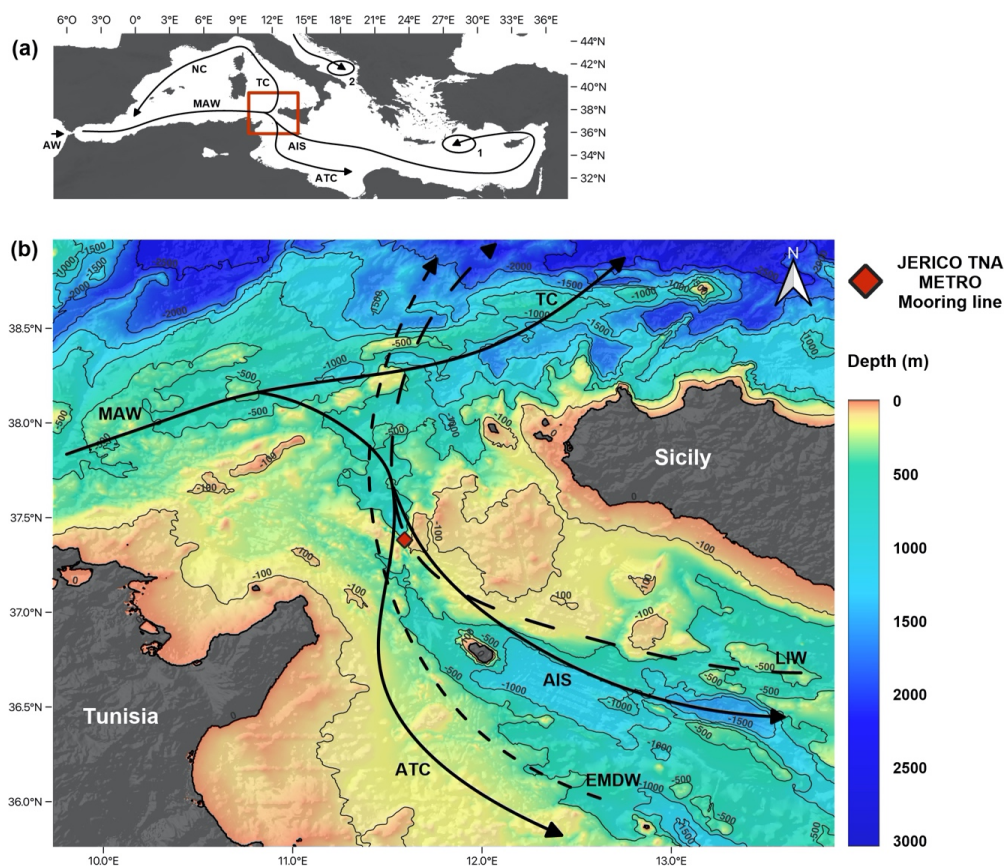
125 The Mediterranean is an elongated, semi-enclosed sea with an anti-estuarine circulation. The
126 Mediterranean Sea is a concentration basin (Bethoux et al., 1999) in which the evaporation exceeds
127 the freshwater inputs, forcing a negative hydrological balance (Robinson and Golnaraghi, 1994). This
128 negative balance is compensated by the entrance of surface oceanic water from the Atlantic Ocean
129 through the Strait of Gibraltar. The colder and nutrient richer Atlantic Waters (AW) spread eastward
130 into the Mediterranean basin (Millot, 1991), where they progressively become warmer, saltier and
131 more oligotrophic as they mix with resident waters (Modified Atlantic Waters – MAW. Also known
132 as Atlantic Waters – AW). MAW circulate following a cyclonic circuit along the Algerian coast
133 (Algerian Current – AC) (Malanotte-Rizzoli et al., 2014; Millot, 1999) and divide into two main
134 branches at the entrance of the Sicily Strait (Figure 1a). One of these branches spreads into the
135 northwestern part of the basin, into the Tyrrhenian Sea, where it continues its path cyclonically. The
136 second branch flows south of Sicily into the Ionian Sea (Lermusiaux and Robinson, 2001). In the Sicily
137 channel itself, the water masses are split again in two different streams (Béranger et al., 2004): (i)
138 the Atlantic Tunisian Current (ATC) that flows to the southeast following the African coast; and (ii)
139 the Atlantic Ionian Stream (AIS) that flows into the deep eastern part of the basin (Figure 1b) and
140 contributes to the MAW transport in the eastern Mediterranean (Jouini et al., 2016; Lermusiaux and
141 Robinson, 2001).

142 The Sicily Strait is located in the central Mediterranean (Figure 1a) and acts as a sill that
143 topographically separates the western and eastern Mediterranean basins. The circulation through
144 the Sicily Strait is characterized by water masses that flow in opposite directions at different depths
145 of the water column (Béranger et al., 2004). The Levantine Intermediate Water (LIW), which enters
146 the strait from the Ionian Sea, occupies the deeper part of the water column along with occasional
147 thin Eastern Mediterranean Deep Water layers (Gasparini et al., 2005; Lermusiaux and Robinson,
148 2001). The Ionian Water (IW) can be present at intermediate depths (Figure 1), while the MAW
149 cover the surface to subsurface part of the water column (Warn-Varnas et al., 1999). Temperature
150 and salinity range from 15-17 °C and 37.2-37.8 psu for the MAW, 15-16.5 °C and 37.8-38.4 psu for
151 the IW and 13.7-13.9°C and 38.7-38.8 psu for the LIW (Astraldi et al., 2002; Bouzinac et al., 1999;
152 Robinson et al., 1999). Lastly, it is important to note, that the surface circulation in the Sicily Strait
153 presents a large seasonal variability concerning the water masses distribution (Béranger et al., 2004;
154 Lermusiaux and Robinson, 2001). Surface circulation experiences a substantial seasonality in the
155 Sicily Strait: during late autumn to late spring, the MAW dominate the surface circulation, allowing
156 nutrient and chlorophyll-enriched waters to enter the strait (Astraldi et al., 2002; D’Ortenzio, 2009).
157 In turn, summer and autumn are dominated by LIW waters. Deep-water circulation remains
158 relatively stable on a seasonal scale (Béranger et al., 2004) with a continuous LIW presence over the
159 year. Finally, during summer, an upwelling settles in the Sicily Strait, allowing the impoverished LIW
160 to reach the surface (Lermusiaux and Robinson, 2001).

161 Regarding its nutrient distributions, the Mediterranean Sea is generally considered an oligotrophic
162 to ultraoligotrophic sea (Krom et al., 1991). However, this oligotrophy is not homogenous and
163 displays a clear west-to-east gradient which is reflected in the nutrient concentration and algal
164 biomass accumulation derived from colour remote sensing (Navarro et al., 2017; Siokou-Frangou et



165 al., 2010). The eastern part of the Mediterranean is considered to be more nutrient depleted than
166 the western part of the basin (Krom et al., 2005; Raimbault et al., 1999), with N:P ratios around 50:1
167 (Krom et al., 2005). At times of maximum annual algal concentration, primary productivity (PP) in
168 the Levantine Basin reaches values of ca. $0.1 \text{ g C m}^{-2} \text{ d}^{-1}$ (Hazan et al., 2018). This value is substantially
169 lower than those recorded in the high productivity regions of the western basin such as the Gulf of
170 Lions, ca. $0.4\text{-}0.65 \text{ g C m}^{-2} \text{ d}^{-1}$ (Gaudy et al., 2003; Rigual-Hernández et al., 2012), or the Alboran Sea,
171 ca. $0.3\text{-}1.3 \text{ g C m}^{-2} \text{ d}^{-1}$ (Bárcena et al., 2004; Morán and Estrada, 2001) during the corresponding
172 period.



173 **Figure 1.** (a) Mediterranean Sea general surface circulation (Astraldi et al., 2002; Béranger et al., 2004;
174 Incarbona et al., 2011; Macias et al., 2019) and location of the study zone. The ellipses show the deep-
175 water formation zones for the LIW (1) and the EMDW (2). (b) Regional oceanographic and geographic
176 setting of the Sicily Strait. The red diamond represents the location of the JERICO TNA METRO mooring
177 line in which the C01 sediment trap is located. Black continuous lines represent surface circulation, while
178 dashed lines show deep-water circulation. The difference in the dashed lines period stands for the
179 occasional aspect of the EMDW. The topographic model was downloaded from the GEBCO database.
180

181
182

3. Material and methods



183

184 **3.1. Field experiments**

185 The C01 sediment trap is part of the JERICO TNA METRO mooring line (Figure 1b) which is
186 maintained by ISMAR-CNR in the Sicily Channel (37.38°N, 11.59°E) thanks to TransNational Access
187 activity in the FP7 JERICO project (Mediterranean sediment Trap Observatory). The mooring line
188 was equipped with a sediment trap located 413 m below the sea surface in a water column of
189 around 450 m deep. The sediment trap was a PPS3/3 model, conical in shape with a 2.5
190 height/diameter ratio and equipped with 12 sampling cups. Further information about this sediment
191 trap configuration and model can be found in Heussner et al., (2006, 1990).

192 Here we present data from November 2013 to mid-October 2014. The sampling period was 15 to
193 16 days from November 2013 to July 2014 and from September 2014 to October 2014. Between
194 July 2014 and September 2014, the sampling was set to 31 days. Before deployment and to limit the
195 degradation of the material caught, sampling cups from both mooring lines were filled with a 5%
196 formalin solution prepared with 40% formaldehyde mixed with 0.45 µm filtered seawater. The
197 solution was then buffered with sodium borate to keep the pH stable and avoid the dissolution of
198 carbonate.

199

200 **3.2 Processing of sediment trap samples**

201 After the recovery, the cups were stored at 2-4°C until their processing. First, the few swimmers
202 that entered the trap were removed with a 1 mm nylon mesh for the big individuals. Then, the
203 formaldehyde was removed by centrifugation and the cup samples were freeze-dried and weighted.
204 A total of 19 samples from the sediment trap were processed for micropaleontological analyses in
205 the micropaleontology laboratory of the Geology department at the University of Salamanca. The
206 samples consisted of aliquots of 1/6 of the original mooring line cups and were preserved in
207 seawater, with a pH between 7.6 and 7.8. All samples were first wet sieved to separate the <63µm
208 fraction and then dry sieved to separate the 63-150 and >150 µm fractions. The washing was carried
209 out with a potassium phosphate-buffered solution (pH= 7.5) to prevent carbonate dissolution.

210

211 **3.3 Planktic foraminifera identification, flux calculations and imaging**

212 The planktic foraminifera identification (Plate 1) and counting to the species level were carried out
213 in the >150 µm fraction using a microscope (Leica Wild M3B). To have a representative picture of
214 the planktic foraminifera population, the complete samples were analyzed (i.e. no splits were
215 applied). Identification was carried out according to Schiebel and Hemleben, (2017). A total of 15
216 species were identified (Plate 1): *Globigerinella siphonifera*, *G. calida*, *Globigerinoides sacculifer*, *G.*
217 *ruber*, *G. ruber* (pink), *Globoturborotalita tenella*, *G. rubescens*, *Orbulina universa*, *Globorotalia*
218 *truncatulinoidea*, *G. inflata*, *G. scitula*, *Globigerina bulloides* (+ *G. falconensis*), *Neogloboquadrina*
219 *incompta* and *Turborotalita quinqueloba* (Plate 1). In addition, benthic foraminifera shells were
220 identified to the lowest taxonomic level possible and counted.

221 The foraminifera fluxes were calculated according to the following formula:

222

$$PF \text{ (shells } m^{-2} d^{-1}) = \frac{(N \times \text{aliqu.}) \times SD^{-1}}{0.1256}$$



223

224 “PF” stands for planktic foraminifera, “N” accounts for the number of individuals identified, “aliq.”
225 refers to the aliquot (1/6 for all samples) and “SD” represents the sampling interval that the
226 sediment trap cup stayed open. Relative abundance for each species was also calculated for all
227 samples.

228 To showcase the species collected by the traps (Plate 1), foraminifera imaging was carried out using
229 a Nikon SMZ18 stereomicroscope equipped with a Nikon DS-Fi3 camera and the image processing
230 software NISElements (version 5.11.03).

231

232 **3.4 Environmental and planktic foraminifera data**

233 To assess the possible relationship of planktic foraminifera fluxes with environmental variability, key
234 environmental parameters, namely satellite-derived chlorophyll-*a* and Sea Surface Temperatures
235 (SSTs) were retrieved from global data sets. Satellite-derived chlorophyll-*a* concentration (mg m^{-3})
236 were obtained from MODIS L3m satellite through NASA’s Giovanni web interface with an 8-day and
237 4 km resolution for a $0.2 \times 0.2^\circ$ area around the mooring location between 01/10/2013 to
238 01/11/2014. Additionally, sea surface temperature SST ($^\circ\text{C}$) were also obtained from the same site
239 with the same resolution to use as a proxy for water temperature and water column stratification.
240 Additionally, to put into context our observations with the regional variability of planktic
241 foraminifera communities in the Mediterranean Sea, modern planktic foraminifera flux datasets
242 were retrieved from different sites. Levantine basin foraminifera fluxes (LevBas) were obtained from
243 Avnaim-Katav et al., (2020), the Gulf of Lions ones (LCD and PLA) from Rigual-Hernández et al.,
244 (2012) and finally the Alboran Sea fluxes (ALB 1F and ALB 5F) from both Bárcena et al., (2004) and
245 Hernández-Almeida et al., (2011). All the foraminifera fluxes concerned the $>150 \mu\text{m}$ fraction,
246 except the ones from the Levantine basin, which represented the $>125 \mu\text{m}$ fraction (Figure 6).

247 Finally, core-top data from the ForCenS database (Siccha and Kucera, 2017) was used to compare
248 the planktic foraminifera abundance patterns from the C01 sediment trap with the seabed
249 sediment. Only seabed sediment located on a 2.5 degree difference in both latitude and longitude
250 was selected to compare our data with sites in the vicinity of the Sicily Strait. This corresponded to
251 a total of 16 core-tops part of the MARGO database. The complete details of the latter can be found
252 in the Supplementary data.

253

254 **3.5 Statistical analysis**

255 To have uninterrupted monthly and daily values from NASA’s Giovanni environmental parameters
256 that coincide with the mean sampling date from the sediment traps, a daily resampling has been
257 carried out using QAnalySeries software.

258 Pearson correlation and *p*-value tests were carried out with the Past4 program. A $p < 0.05$ was used
259 to denote statistical significance.

260 In addition, a canonical correspondence analysis (CCA) was also used to estimate the influence of
261 both SST and chlorophyll-*a* on foraminifera fluxes. A CCA is a correspondence analysis of a species
262 matrix where each site has given values for one or more environmental variables (SST and
263 chlorophyll-*a* concentration in this case). The ordination axes are linear combinations of the



264 environmental variables. A CCA is considered an example of direct gradient analysis, where the
265 gradient in environmental variables is known and the species abundances/fluxes are considered to
266 be a response or to be affected by this gradient (Nielsen, 2000).

267 Additionally, to evaluate the magnitude of the foraminifera fluxes across major regions of the
268 Mediterranean, an estimation of the annual planktic foraminifera flux (shells $\text{m}^{-2} \text{y}^{-1}$) was calculated
269 using the sediment trap data from the literature review and our study. To that purpose, the data
270 was annualized according to the following formula:

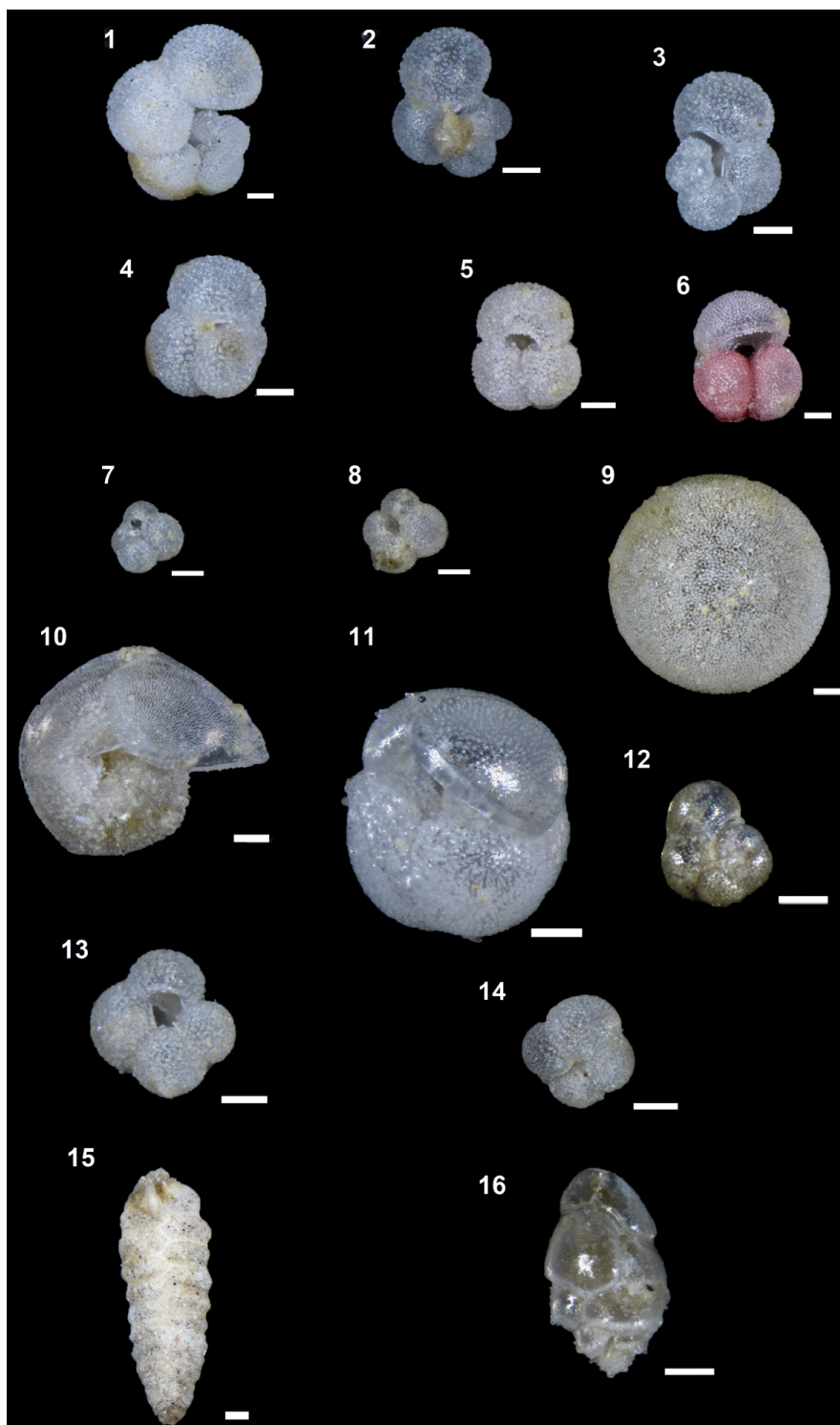
$$271 \quad \text{Annual PFF} = \sum(PF \times SD + cPF \times mSD)$$

272 Where “PFF” stands for planktic foraminifera flux (shells $\text{m}^{-2} \text{d}^{-1}$), “SD” accounts for sampling days,
273 “cPF” represents calculated planktic foraminifera flux (shells $\text{m}^{-2} \text{d}^{-1}$) and “mSD” stands for missing
274 sampling days. “cPF” calculation depended on the site. For the datasets retrieved from the Sicily
275 Strait and the Levantine basin, less than 20 sampling days were missing, so the corresponding
276 planktic foraminifera fluxes were replaced by the mean of the first and last flux values recorded.
277 The two datasets from the Alboran Sea displayed more than 70 missing days, so the corresponding
278 flux values used were a mean of the two closest months to the missing data. Concerning the two
279 time series from the Gulf of Lions, they covered more than one year. Therefore, a mean year was
280 estimated: a mean monthly flux value was calculated for all 12 months based on all the available
281 measurements and then multiplied by the corresponding mean duration of each month, and then,
282 all monthly fluxes were added together.

283 To compare the species richness and diversity across the previously described sites, Simpson (D) and
284 Shannon/Weiner (H/W) indexes were calculated. Here, we reported the inverse Simpson index (1-
285 D). None of these indexes were calculated for the Alboran Sea sites (ALB 1F and ALB 5F) because
286 only information about the four main species was documented (Bárcena et al., 2004; Hernández-
287 Almeida et al., 2011).

288 Finally, the squared chord distance (SCD) between the C01 sediment trap and every core top sample
289 downloaded from the ForCenS database (Siccha and Kucera, 2017) planktic foraminifera relative
290 abundance was calculated. It is a widely used metric in palaeoecological and paleontological studies
291 as it is the most effective index for identifying the closest analogues in planktic foraminifera
292 datasets (Prell, 1985). This is mainly because it shows the best balance in weighing the contribution
293 of abundant and rare species in a given association (Jonkers et al., 2019). In this study, SCD values
294 lower than 0.25 have been considered as reliable analogues (Ortiz and Mix, 1997).

295





297 **Plate 1.** Planktic (1-14) and the most common benthic foraminifera (15-16) species collected from the
 298 C01 sediment trap. The white scale bars on all figures represent 100 μm . (1) *G. siphonifera*, side view. (2)
 299 *G. calida*, umbilical view. (3) *G. calida*, apertural view. (4) *G. sacculifer*, umbilical view. (5) *G. ruber*,
 300 umbilical view. (6) *G. ruber* (pink), umbilical view. (7) *G. tenella*, umbilical view. (8) *G. rubescens*, umbilical
 301 view. (9) *O. universa*. (10) *G. truncatulinoides*, umbilical view. (11). *G. inflata*, apertural view. (12) *G.*
 302 *scitula*, umbilical view. (13) *G. bulloides*, umbilical view. (14) *N. incompta*, umbilical view. (15) *Textularia*
 303 *spp.* (16) *Bulimina marginata*, apertural view.

304

305 4. Results

306

307 4.1 General considerations of the planktic foraminifera assemblages

308

309 **Table 1.** Counts and key statistics of the planktic foraminifera species and the benthic foraminifera group
 310 from the > 150 μm fraction identified in the 19 sediment trap cups of the JERICO site. Mean, maximum
 311 (Max), minimum (Min), standard deviation (SD) of the relative abundance and fluxes. Raw counts also
 312 include a total and % of the total description.

	<i>G. siph.</i>	<i>G. cal.</i>	<i>G. sacc.</i>	<i>G. rub.</i>	<i>G. rub. (p.)</i>	<i>G. ten.</i>	<i>G. rubesc.</i>	<i>O. univ.</i>	<i>G. truncat.</i>	<i>G. inf.</i>	<i>G. sci.</i>	<i>G. falco.</i>	<i>G. bull.</i>	<i>N. inc.</i>	<i>T. quin.</i>	Benthics	Total planktic
COUNTS (N)																	
Mean	2.5	3.1	4.1	6.5	5.2	1.1	3.7	3.9	37.0	109.2	1.3	0.1	16.2	1.5	0.5	7.4	195.9
Max	6	11	10	22	40	5	9	15	118	456	7	1	111	8	3	42	633
Min	0	0	0	1	0	0	0	0	1	1	0	0	0	0	0	1	14
SD	1.8	2.8	3.2	5.6	9.2	1.5	2.5	4.1	33.2	132.5	2.3	0.2	26.4	2.3	1.1	9.2	
Total	48	59	78	124	99	21	71	74	703	2075	24	1	307	29	10	141	3723
% of total	1.3	1.6	2.1	3.3	2.7	0.6	1.9	2.0	18.9	55.7	0.6	0.0	8.2	0.8	0.3	3.6	
ABUNDANCES (%)																	
Mean	2.0	2.7	2.8	5.5	5.7	0.9	4.0	3.0	20.5	41.6	1.9	0.1	7.3	1.8	0.2	5.2	
Max	7.4	10.2	8.1	16.0	32.5	8.5	14.3	16.9	46.1	72.0	8.8	1.6	26.7	21.4	1.7	12.5	
Min	0.0	0.0	0.0	0.5	0.0	0.0	0.0	0.0	7.1	1.6	0.0	0.0	0.0	0.0	0.0	0.6	
SD	2.0	2.7	2.4	4.7	10.1	1.9	4.3	3.9	9.0	24.0	3.2	0.4	6.5	4.8	0.4	3.9	
FLUXES (shells $\text{m}^{-2} \text{d}^{-1}$)																	
Mean	7.9	10.2	13.2	19.6	15.8	3.6	12.0	11.0	113.8	354.9	3.3	0.2	57.2	5.3	1.8	24.8	629.8
Max	26.1	47.8	34.7	65.7	127.4	21.7	28.7	35.0	368.5	1361.5	22.3	3.2	482.0	34.7	13.0	182.4	1889.9
Min	0.0	0.0	0.0	3.2	0.0	0.0	0.0	0.0	3.2	3.2	0.0	0.0	0.0	0.0	0.0	3.0	44.6
SD	6.5	11.1	11.3	17.7	29.6	5.8	8.6	10.7	107.2	426.4	6.3	0.7	110.7	8.8	3.9	39.9	

313

314 A total of 3723 planktic foraminifera shells and 141 benthic foraminifera were counted. Planktic
 315 foraminifera were identified at the species level, resulting in a total of 15 different species identified
 316 (Plate 1). A mean of 196 planktic foraminifera specimens per sample were identified, with a
 317 minimum of 14 individuals in November 2013 and a maximum of 633 individuals in mid-March 2014
 318 (Table 1).

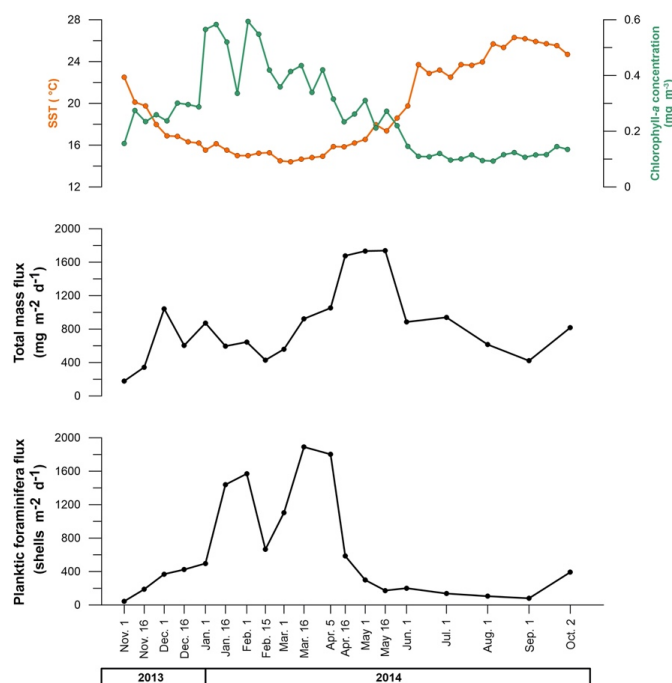


319 According to the raw counts results, the most abundant species was *G. inflata*, which represented
320 55.7% of the total planktic foraminifera individuals. The second most represented species was *G.*
321 *truncatulinoidea*, with 18.9%, followed by *G. bulloidea* with 8.2%. These three species alone
322 accounted for more than 80% of the planktic foraminifera identified. The remaining species
323 abundances were below 5%. *G. ruber*, *G. ruber* (pink), *O. universa*, *G. rubescens* and *G. sacculifer*
324 represented between 2 and 3.3 % of the total individuals. Species like *G. tenella*, *G. scitula*, *N.*
325 *incompta* and *T. quinqueloba* were very scarce and accounted individually for less than 1% of the
326 total planktic individuals (Table 1). Note that *G. inflata*, *G. truncatulinoidea* and *G. ruber* were the
327 only species present in all samples.

328

329 4.2 Total mass and planktic foraminifera fluxes

330



331

332 **Figure 2.** Total mass flux (TMF) (mg m⁻² day⁻¹), total planktic foraminifera flux (PFF) (shells m⁻² day⁻¹), SST
333 (°C) and chlorophyll-a concentration (mg m⁻³) changes between November 2013 and October 2014.

334

335 The mean total mass flux for the whole period of the study was 772.5 mg m⁻² d⁻¹, with a maximum
336 value of 1737.7 mg m⁻² d⁻¹ and a minimum value of 179.5 mg m⁻² d⁻¹ reached in mid-May 2014 and
337 November 2013 respectively (Figure 2). Higher total mass flux values were reached during spring
338 2014, while lower values appeared during both autumn 2013 and 2014.

339 Planktic foraminifera mean flux across the interval studied was 629.8 shells m⁻² d⁻¹ with a maximum
340 value of 1889.9 shells m⁻² d⁻¹ and a minimum of 44.6 shells m⁻² d⁻¹ reached in mid-March 2014 and
341 in November 2013 respectively. Higher values occurred during two periods, early spring and winter



342 2014, while the lower ones occurred from late spring to fall 2014. Overall, the seasonal mean values
343 were 1194.3 shells $\text{m}^{-2} \text{d}^{-1}$ for the winter period, 612.3 shells $\text{m}^{-2} \text{d}^{-1}$ for spring, 283.5 shells $\text{m}^{-2} \text{d}^{-1}$
344 for autumn and finally 107.2 shells $\text{m}^{-2} \text{d}^{-1}$ for summer.

345 SST mean value was 19.2 °C and values ranged between a maximum of 26.1 and a minimum of 14.5
346 °C. The mean chlorophyll-*a* value was 0.27 mg m^{-3} , the maximum value displayed was 0.56 mg m^{-3}
347 while the minimum one was 0.09 mg m^{-3} (Figure 2).

348

349 **4.3 Foraminifera species fluxes**

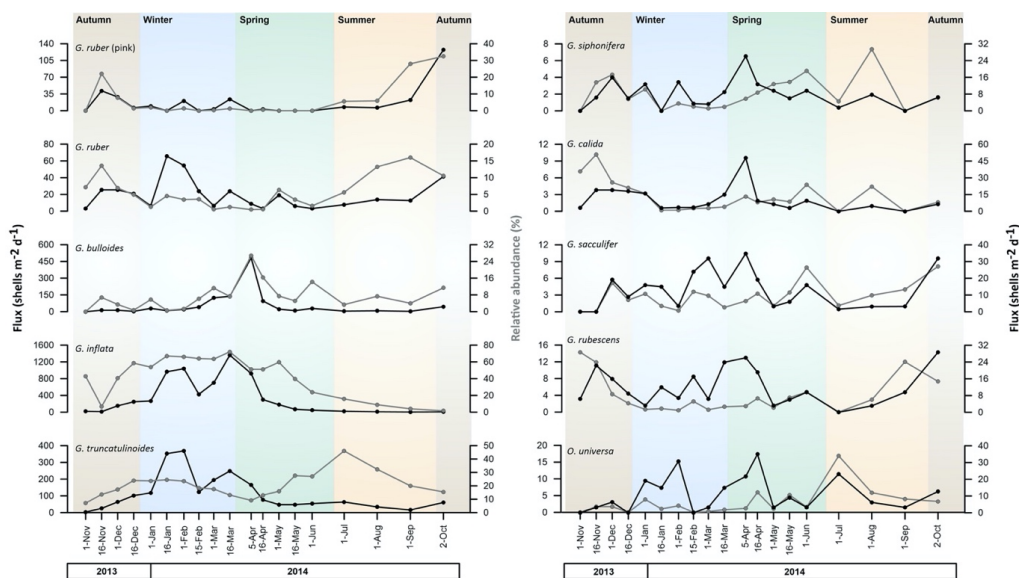
350 Overall, most of the planktic foraminifera species collected by the trap exhibited either a uni-modal
351 or bi-modal flux distribution with a few exceptions (Figure 3).

352 *Globorotalia inflata* exhibited the highest fluxes of all species, with a mean flux of 368 shells $\text{m}^{-2} \text{d}^{-1}$
353 throughout the record, with peak values in mid-March 2014 (1361 shells $\text{m}^{-2} \text{d}^{-1}$) and minimum in
354 November 2013 (3 shells $\text{m}^{-2} \text{d}^{-1}$). *G. truncatulinoides* was the second most important contributor
355 (mean of 114 shells $\text{m}^{-2} \text{d}^{-1}$), with a maximum in mid-February and a minimum in November 2013
356 (368 and 3 shells $\text{m}^{-2} \text{d}^{-1}$, respectively). *G. bulloides* was the third most important contributor to the
357 total planktic foraminifera fluxes with a mean flux of 57.2 shells $\text{m}^{-2} \text{d}^{-1}$ and maximum values
358 registered in April 2014 and minima in November 2013 (482 and 0 shells $\text{m}^{-2} \text{d}^{-1}$, respectively).

359 The remaining species displayed mean fluxes lower than 50 shells $\text{m}^{-2} \text{d}^{-1}$. *G. calida*, *G. ruber*, *G. ruber*
360 (pink), *G. rubescens* and *O. universa* mean fluxes were comprised between 10 and 20. Among these
361 species, *G. ruber* and *G. ruber* (pink) stood out and showed maximum fluxes of 66 shells $\text{m}^{-2} \text{d}^{-1}$ in
362 February 2014 and 127 shells $\text{m}^{-2} \text{d}^{-1}$ in October 2014, respectively. The remaining species, *G.*
363 *siphonifera*, *G. scitula*, *G. falconensis*, *N. incompta* and *T. quinqueloba* mean and maximum fluxes
364 were lower than 10 and 35 shells $\text{m}^{-2} \text{d}^{-1}$, respectively, thereby representing a low contribution to
365 the total foraminifera fluxes.

366 Finally, it is worth noting that benthic foraminifera were also collected by the trap, displaying a mean
367 flux of 25 shells $\text{m}^{-2} \text{d}^{-1}$. The peak contribution of these taxa was recorded in April 2014 (182 shells
368 $\text{m}^{-2} \text{d}^{-1}$), and a minimum value in January 2014 (3 shells $\text{m}^{-2} \text{d}^{-1}$).

369



370
 371 **Figure 3.** Planktic foraminifera fluxes (shells $m^{-2} d^{-1}$, black lines) and relative abundances (% , grey lines)
 372 from November 2013 to October 2014 of the 10 most abundant species identified. Note that the scale
 373 of the fluxes and abundances depend on the species. Background colour filling represents the different
 374 seasons: brown for autumn, blue for winter, green for spring and orange for summer.

375
 376 The variations in relative abundance differed according to the species. Most of the species displayed
 377 a unimodal distribution across the studied interval (Figure 3), with some exceptions such as *G.*
 378 *siphonifera*, *G. calida* or *G. ruber*.

379 Overall, *G. inflata* dominated the association from late autumn until mid-spring. Its relative
 380 abundance was comprised between 72% reached in mid-March 2014 and around 2% in mid-
 381 November 2013 (Figure 3). *G. truncatulinoides* relative abundance pattern was different from any
 382 other species. The lowest relative abundance was reached in November 2013: around 7%, while the
 383 highest abundance was 46% in July 2014. Note that despite the seasonality of its abundance, the
 384 amplitude of its relative abundance change was low compared to other species (Figure 3). In turn,
 385 the third most abundant foraminifera species, *G. bulloides*, displayed a pronounced seasonal change
 386 in its relative abundance reaching values up to 27% in early spring (April 2014) and dropping to
 387 about 5-8% in November 2014.

388 Secondary contributors, such as *G. siphonifera* and *G. sacculifer* reached their maximum
 389 contributions (~8%) in August and June 2014, respectively, *G. calida* in mid-November 2013 (10%),
 390 *G. ruber* in November 2013 (16%), *G. ruber* pink in October 2014 (32.5%) and both *G. rubescens* and
 391 *O. universa* exhibited their maximum contributions (with 14-15% for both species) in November
 392 2013 and in July 2014, respectively.

393 Overall, *G. inflata* is the only species that displayed its maximum mean relative abundance during
 394 winter: 64%. *G. siphonifera*, *G. sacculifer*, and *G. bulloides*, maximum mean relative abundances
 395 were reached during spring: 3%, 3.5%, 14% respectively. *G. calida*, *G. tenella*, *G. rubescens* and *N.*
 396 *incompta* maximum mean abundances appeared to be in autumn: 5.7%, 2.2%, 8% and 4.8%

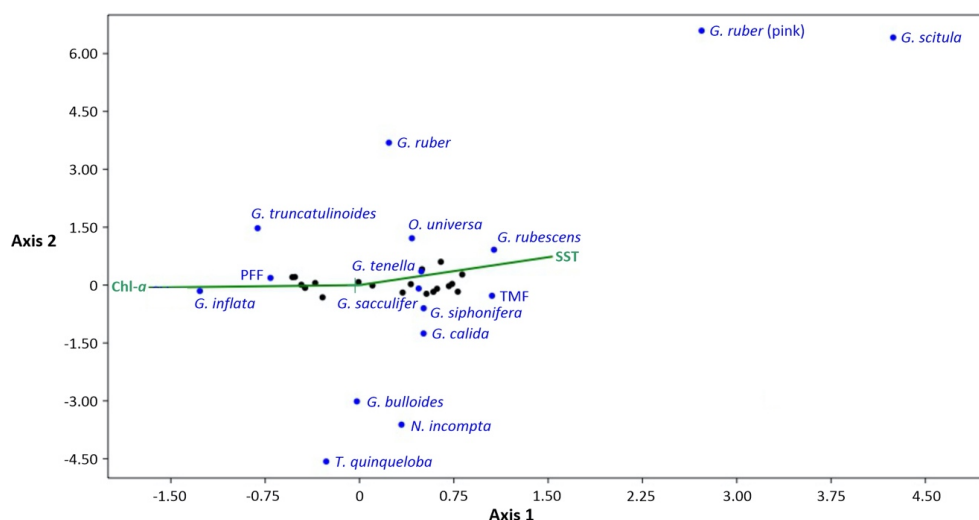


397 respectively. Finally, *G. ruber*, *G. ruber* (pink), *O. universa*, *G. truncatulinoides* and *G. scitula*
398 maximum mean relative abundances were displayed in summer: 11.6%, 13.2%, 8.9%, 32.8% and
399 6.4% respectively.

400

401 4.4 Chlorophyll-*a* and SST impact on foraminifera fluxes

402



403

404 **Figure 4.** CCA analysis of all the planktic foraminifera species flux with the SST (°C) and the chlorophyll-*a*
405 (“chl-*a*” in the CCA, in mg m⁻³) as the explanatory variables. The total mass flux (“TMF”) and planktic
406 foraminifera flux (“PFF”) are also included. Black dots represent the 19 sediment trap samples studied.

407

408 A CCA (see section 3.4) was carried out to characterize the impact of both the SST and the
409 chlorophyll-*a* on the planktic foraminifera fluxes (Figure 4).

410 Total planktic foraminifera flux and the fluxes of *G. inflata* and *G. truncatulinoides* are positively
411 affected by the chlorophyll-*a* concentration and negatively affected by the SST. On the other hand,
412 *G. ruber*, *G. ruber* (pink) and *G. scitula* fluxes showed an opposite pattern, being positively related
413 with the SST and negatively with the chlorophyll-*a* concentration. *O. universa*, *G. rubescens*, *G.*
414 *tenella*, *G. sacculifer*, *G. siphonifera* and *G. calida* fluxes are positively correlated with the SST and
415 negatively with chlorophyll-*a* concentration, nonetheless, the impact of these parameters is weaker
416 compared with the previous species. Finally, *G. bulloides*, *N. incompta* and *T. quinqueloba* fluxes are
417 positively influenced by the chlorophyll-*a* concentration, however, (arguably excepting for *G.*
418 *bulloides*) no clear effect of the SST was displayed on these species fluxes.

419

420 5. Discussion

421

422 5.1 Seasonal variations in the magnitude of planktic foraminifera fluxes in the Sicily Strait

423



424 The strong seasonality in the planktic foraminifera fluxes registered by the trap is generally similar
425 in amplitude to previous studies in the Mediterranean (Bárcena et al., 2004; Rigual-Hernández et
426 al., 2012) and other temperate settings (Rembauville et al., 2016; Wilke et al., 2009), thereby
427 suggesting the CO₁ record mainly reflects the temporal variations in planktic foraminifera
428 abundance in the upper water column. Therefore, next, we discuss the influence of oceanographic
429 controls on the planktic foraminifera fluxes.

430 Our data shows that, despite differences in the magnitude of their fluxes, most of the species
431 identified display their maximum flux during winter, winter/spring transition or spring (Figure 3)
432 thereby coinciding with the period of maximum algal biomass accumulation and coldest SSTs (Figure
433 2). The enhanced primary productivity during winter and spring is mostly related to an
434 intensification of the chlorophyll-*a* and nutrient richer MAW flow into the Eastern Mediterranean
435 basin (D'Ortenzio, 2009; Siokou-Frangou et al., 2010). Our CCA results (Figure 4) show that, although
436 the flux patterns increase during winter and spring, only the planktic foraminifera flux, *G. inflata*, *G.*
437 *truncatulinoides* and arguably *G. bulloides* (further discussed below) fluxes are negatively related to
438 SSTs and positively with the chlorophyll-*a* concentration. The dominance of the planktic
439 foraminifera fluxes by these three species and their affinity for mesotrophic waters is not surprising
440 as *G. inflata* and *G. truncatulinoides* are typically associated with the MAW, winter water mixing
441 events and hydrologic fronts in the western Mediterranean, while *G. bulloides* is generally
442 associated with eutrophic environments linked to upwelling conditions (Azibeiro et al., 2023).
443 Overall, these three taxa have been described to be dominant during winter in various western
444 regions of the Mediterranean, such as the Alboran Sea (Bárcena et al., 2004; Hernández-Almeida et
445 al., 2011), the Provençal basin and in the Gulf of Lions (Pujol and Grazzini, 1995; Rigual-Hernández
446 et al., 2012). Interestingly *G. inflata*, *G. truncatulinoides* and *G. bulloides* are almost absent in the
447 eastern part of the basin, most likely due to the low algal biomass accumulation (Avnaim-Katav et
448 al., 2020; Thunell, 1978).

449 Conversely, species such as *G. ruber*, *G. ruber* (pink), *G. scitula*, *G. rubescens* and *G. sacculifer* display
450 their maximum fluxes in summer or autumn (Figure 3). During the warm periods, summer and
451 autumn, the eastward advection of Atlantic waters in the Sicily Strait is weakened due to an
452 increased meandering of the ATC (Figure 1) and the local hydrography patterns (Béranger et al.,
453 2004), leading to a local water column stratification period which is also well documented in the
454 whole Mediterranean basin during summer (Siokou-Frangou et al., 2010). This translates into a
455 reduced MAW influence, and a larger influence of the LIW at intermediate depths (Astraldi et al.,
456 2002, 2001; Jouini et al., 2016). Therefore, the water column becomes warmer, saltier and more
457 nutrient depleted than the general conditions of the western basin (Gasparini et al., 2005; Navarro
458 et al., 2017; Siokou-Frangou et al., 2010) and provides the necessary environmental and
459 oceanographical configuration for eastern basins taxa to develop or being transported from the
460 easternmost part of the Mediterranean. Indeed, our CCA results (Figure 4) support these
461 observations (Figure 3). The latter species have been described to reach their maximum abundances
462 in the eastern part of the Mediterranean, specifically in the Ionian and Levantine basins during both
463 summer and autumn (Avnaim-Katav et al., 2020; Pujol and Grazzini, 1995).

464 Some species, such as *O. universa* or *G. calida*, do not display a clear flux pattern over the period
465 studied. CCA results suggest that these species have an affinity for warm and less productive



466 conditions. These taxa are considered widespread in the Mediterranean basin, although their
467 relative contributions are generally higher in the eastern part of the basin (Avnaim-Katav et al.,
468 2020; Pujol and Grazzini, 1995; Thunell, 1978). Lastly, it is important to note that the low number of
469 specimens of *G. falconensis*, *N. incompta*, *T. quinqueloba* and *G. tenella* found in our samples, makes
470 the estimation of shell fluxes for these species unreliable. These results are not surprising, since *N.*
471 *incompta* is mainly found in the northwestern part of the basin owing to cold and eutrophic
472 conditions (Azibeiro et al., 2023; Millot and Taupier-Letage, 2005) while *T. quinqueloba* has generally
473 been associated to cool Atlantic waters or cool marginal seas (Azibeiro et al., 2023).

474 The record of benthic foraminifera (Figure 3) indicates that the trap also collected resuspended
475 sediments. The main benthic species identified were *T. saggitula* spp. and *B. marginata* (Plate 1)
476 which are considered infaunal species, i.e. they live buried in the sediment (Balestra et al., 2017;
477 Milker and Schmiedl, 2012) and are commonly found in continental shelves and slopes. Overall,
478 benthic foraminifera accounted only for a mean of 3.4% of the total foraminifera identified in the
479 C01 sediment trap (Table 1) and the % of planktic oscillated between 87.5 and 99.4%. Therefore, it
480 can be assumed that the C01 mooring line recorded mainly a pelagic signal.

481 In summary, planktic foraminifera flux was maximum during winter and spring, coinciding with the
482 maximum seasonal eastward advection that brings MAW further east into the Sicily Strait. These
483 waters are less saline and nutrient enriched compared to the easternmost waters from the
484 Levantine basin. *G. inflata*, *G. truncatulinooides* and *G. bulloides* (the three most abundant species
485 that dominate the PFF), which are species described to come from the western basins, are probably
486 brought by the MAW and then dominate the planktic foraminifera population. On the other hand,
487 during summer and autumn, the eastward advection weakens, allowing the LIW and AIS to
488 dominate the surface circulation due to the water column stratification and set favourable
489 conditions for eastern basin dominant taxa such as both morphotypes of *G. ruber*, *G. rubescens*, *G.*
490 *sacculifer*. This results in a significantly decreased planktic foraminifera flux due to the absence of
491 western basin dominant species.

492

493 **5.2 Species succession, ecology and impact of the SST and chlorophyll-*a***

494 The annual planktic foraminifera assemblage collected by the C01 trap reflects a diverse planktic
495 foraminifera assemblage with species with contrastingly different ecological preferences,
496 encompassing a wide range of depth habitats and diverse feeding strategies. Overall, the annual
497 assemblage composition agrees well with previous ship-board observations (Pujol and Grazzini,
498 1995) in the Strait of Sicily during VICOMED 1988 cruise, where *G. inflata*, *G. truncatulinooides* and
499 *G. bulloides* were documented as the most abundant taxa.

500 Next, we discuss the ecology of the most abundant species and the impact of chlorophyll-*a* and SST
501 on their distribution. We also discuss the foraminifera groups suggested by Jonkers and Kučera,
502 (2015), to explore their correlation with the previous parameters on an interannual scale. The latter
503 work proposed 3 groups: group 1 is formed by tropical and subtropical species, group 2 consists of
504 temperate to subpolar taxa, and group 3 represents the deep-dwelling species. These groups were
505 described as a result of the seasonal maximum fluxes timing of each species and their relationship
506 with both temperatures and nutrients (amongst other parameters) in different time-series across



507 the world ocean. Therefore, here we also used this grouping to compare and complete this
508 classification from a new time-series dataset.

509 *Globorotalia inflata* is the most abundant taxon in our samples. Our data shows that maximum
510 fluxes and relative abundances of this species are reached during winter and the winter-spring
511 transition (Figure 3). The relative abundances showed strong positive and negative significant (p
512 <0.05) correlations with the chlorophyll-*a* concentration and the SST: 0.808 and -0.896 respectively
513 (Figure 5). It is a non-spinose species and is considered a deep dweller (Hemleben et al., 1989;
514 Schiebel and Hemleben, 2017). Generally regarded as showing limited opportunistic behaviour and
515 it has been often associated with eddies and hydrological fronts (Chapman, 2010; Retailliau et al.,
516 2011). Concerning the Mediterranean, its maximum stocks and abundances have been recorded
517 along the southern margin of the western Mediterranean basin (Azibeiro et al., 2023), especially
518 during winter (Bárcena et al., 2004; Pujol and Grazzini, 1995; Rigual-Hernández et al., 2012); while
519 it is poorly represented in the eastern part, even absent in the Levantine basin (Avnaim-Katav et al.,
520 2020). As a consequence, *G. inflata* can be considered as a mesotrophic species, which is dominant
521 in regions with some degree of stratification of the water column and an intermediate amount of
522 nutrients and it has been used as a tracer of the Atlantic inflow in the Mediterranean basin (Azibeiro
523 et al., 2023), which agrees with the local hydrography in the Sicily Strait during winter and spring.
524 As *G. inflata* appeared in periods of cool and nutrient enriched waters (Figure 3), which coincide
525 with the periods of higher MAW influence in the Sicily Strait (Béranger et al., 2004), we consider
526 that our results further confirm *G. inflata* as tracer of the MAW in the Sicily Strait.

527 *Globorotalia truncatulinoides* is the second most abundant species in our record. However, our CCA
528 results suggest that the seasonal variations in *G. truncatulinoides* are not directly correlated with
529 either chlorophyll-*a* concentration or SSTs ($r = -0.162$ and 0.256 , respectively, $p > 0.05$) (Figure 5).
530 This highlights the fact that environmental controls other than the ones considered here may be
531 affecting its distribution. This taxon is a cosmopolitan species found in all major oceans (Schiebel
532 and Hemleben, 2017) and is considered a deep dweller with an affinity for water-mixing conditions
533 (Margaritelli et al., 2020; Schiebel and Hemleben, 2005). It is a non-spinose species with a complex
534 life cycle. In the Mediterranean, peak abundances of this species are found in the northwestern part
535 of the basin, where it represents a major component of the assemblages (Pujol and Grazzini, 1995;
536 Rigual-Hernández et al., 2012), while it is absent in the easternmost part of the basin (Avnaim-Katav
537 et al., 2020). This species has been documented to have a complex life cycle and reproductive
538 strategy. *G. truncatulinoides* has been described to reproduce once a year in the upper layers of the
539 water column, generally when the water mixing allows the migration of juvenile individuals to the
540 surface (Lohmann and Schweitzer, 1990; Schiebel et al., 2002). Then, adult individuals migrate
541 downward the water column and spend the rest of their life cycle (Rebotim et al., 2017; Schiebel
542 and Hemleben, 2005). Hence, we speculate that these complex migratory patterns may be playing
543 a role here. As its reproduction cycle is mainly controlled by the gametogenesis process, and as
544 described previously, it reproduces once a year (a slower rate than the majority of the planktic
545 foraminifera species) (Schiebel and Hemleben, 2017), then, although different stages of its life cycle
546 could be affected by SST and chlorophyll-*a*, this is not necessarily registered by the sediment traps
547 in every stage of its growth.



548 *Globigerina bulloides* was the third most abundant planktic foraminifera species identified here. It
549 is a surface to subsurface dweller and one of the most common species across the world ocean
550 (Schiebel and Hemleben, 2017). Interestingly, our analysis showed no significant correlation
551 between changes in *G. bulloides* relative abundance and chlorophyll-*a* concentration or SST ($r =$
552 -0.145 and -0.111 respectively, $p > 0.05$). However, across the time span studied, this taxon showed
553 its maximum abundance and fluxes during relatively high chlorophyll-*a* and cool SST conditions
554 (Figure 3). This highlights that other environmental parameters than the ones considered here might
555 be playing a role in its distribution. It is a spinose species known for its opportunistic feeding strategy
556 (Schiebel et al., 2001) and affinity for upwelling and eutrophic environments (Azibeiro et al., 2023;
557 Bé et al., 1977). Within the Mediterranean Sea, it displays peak export fluxes to the deep sea in
558 areas of high productivity such as the Gulf of Lions and the Alboran Sea during the high productivity
559 period in late winter to spring (Azibeiro et al., 2023; Bárcena et al., 2004; Hernández-Almeida et al.,
560 2011; Rigual-Hernández et al., 2012), while few individuals are found in the eastern part of the
561 Mediterranean (Avnaim-Katav et al., 2020). We surmise that owing to its multiple trophic strategies
562 and its multi-diet characteristics, it could adapt and feed on varying chlorophyll-*a* concentrations.
563 Also, the lack of correlation with both parameters could be explained by the fact that this taxon is
564 associated with eutrophic conditions. In the Sicily Strait, the high productivity period ranges from
565 winter to spring, and the conditions allow deep mesotrophic dwellers (i.e. *G. inflata*) to dominate
566 the assemblage; while in summer and autumn, the upwelling setting brings oligotrophic conditions
567 that are not favourable for this species. In addition, the maximum abundances of *G. bulloides* are
568 displayed coincidentally with the highest number of benthic foraminifera identified (see
569 Supplementary data), which in turn could mean that some of the *G. bulloides* specimens during their
570 maximum abundance have a resuspended origin.

571 *Globigerinoides ruber* and *G. ruber* (pink) were the fourth and fifth most abundant species in our
572 samples (Table 1). Our correlation analyses showed a significant positive effect of SST ($r = 0.803$ and
573 0.678 , $p < 0.05$) and a significant negative effect of chlorophyll-*a* ($r = -0.567$ and -0.464 respectively,
574 $p < 0.05$) on both *G. ruber* and *G. ruber* (pink) respectively (Figure 5). These species have been
575 described as tropical to subtropical taxa, with an affinity for oligotrophic and stratified waters (Bé
576 et al., 1977). Both of these species are among the shallowest dwellers of the extant planktic
577 foraminifera species and are considered one of the most adaptable to varying surface water
578 conditions (Kemle-von Mücke and Oberhänsli, 1999; Schiebel and Hemleben, 2017). Due to its
579 temperature and salinity limits for food acceptance, the white variety is one of the most studied
580 foraminifera species in culture experiments, which highlight their euryhaline and eurythermal life
581 cycle (Bijma et al., 1990; Lombard et al., 2009). In today's ocean, the white variety is substantially
582 more abundant than the pink one (Schiebel and Hemleben, 2017). In the case of the Mediterranean
583 basin, *G. ruber* is generally associated with warm and oligotrophic waters (Pujol and Grazzini, 1995)
584 and is abundant in the eastern oligotrophic basin, where it dominates the assemblages in the
585 Levantine basin during spring and fall (Avnaim-Katav et al., 2020). However, although present in the
586 western basin, its abundance is much lower in the Gulf of Lions (Rigual-Hernández et al., 2012) and
587 in the Alboran Sea (Bárcena et al., 2004). Overall, the correlation data agrees with the previous work
588 that linked *G. ruber* (both varieties) to warm and oligotrophic conditions generally displayed during
589 a higher stratification of the water column (Schiebel et al., 2004) as they appear mainly during



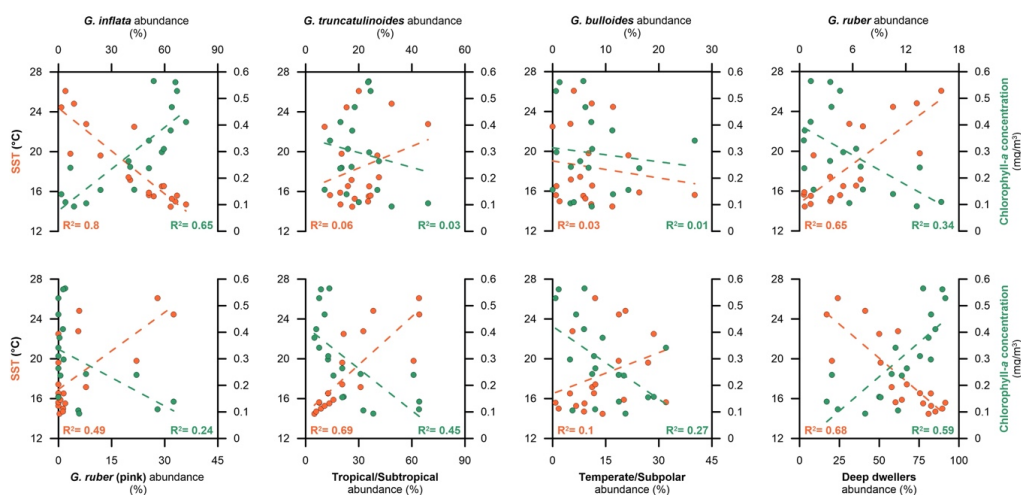
590 summer and autumn, coincidentally with the increased LIW and eastern basin waters influence in the
591 Sicily Strait.

592 According to Jonkers and Kučera, (2015), the foraminifera fluxes can be predicted on a seasonal
593 scale for three different groups of planktic foraminifera. Following this approach, we explore the
594 relative abundance of these three aggrupations to explore if these correlate with both SST and
595 chlorophyll-*a* concentration (see Supplementary Table 1) on the period covered by the sediment
596 trap (Figure 5). The first group (group 1) consists of both *G. ruber* varieties, *G. sacculifer*, *O. universa*,
597 *G. siphonifera*, *G. rubescens* and *G. tenella*. The second group (group 2) is formed by *G. bulloides*, *T.*
598 *quinqueloba*, *N. incompta*, *G. scitula* and *G. calida*. In our record, however, either *G. bulloides* or *G.*
599 *calida* displayed a similar trend, and the remaining three species abundance was <1.5%, making any
600 significant assumption difficult (Table 1). The third (group 3) is composed by the deep dwellers *G.*
601 *inflata* and *G. truncatulinooides*. Group 1 showed a strong and significant positive correlation with
602 the SST (Figure 5) and a negative with the chlorophyll-*a* ($r= 0.828$ and -0.668 respectively, $p < 0.05$,
603 see Supplementary Table 1). This is not surprising as the majority of the group is formed by species
604 not only considered tropical but also well adapted to oligotrophic and nutrient impoverished
605 environments (Chapman, 2010; Hemleben et al., 1989; Schiebel and Hemleben, 2017). In addition,
606 most components of this group are symbiont bearing species (Takagi et al., 2019), which have been
607 described to be more adapted to nutrient depleted and oligotrophic conditions. Group 2 on the
608 other hand did not show any strong correlation to either SST and chlorophyll-*a* concentration,
609 although a significant negative correlation was displayed between the group abundances and the
610 latter parameter ($r= -0.525$, see Supplementary Table 1). This result is not surprising as the main
611 component of this group is *G. bulloides*, which previously showed a lack of correlation with both SST
612 and chlorophyll-*a*, while the remaining species of this group were taxa that tend to be outnumbered
613 by more opportunistic species (i.e. *N. incompta* and *T. quinqueloba*) (Kuroyanagi and Kawahata,
614 2004; Schiebel, 2002). Also, the overall abundance of these taxa was very low in our samples
615 compared to the other two groups, which in turn could affect the correlation results. Here we
616 propose that the mesotrophic conditions of the Sicily Strait developed during the relatively high
617 productivity period are not favourable enough for the development of the taxa comprised in group
618 2. Finally, group 3 displayed a strong and significant positive correlation with chlorophyll-*a*
619 concentration ($r= 0.771$, $p < 0.05$), which is an expected trend according to the affinity showed to
620 mesotrophic conditions by the two species that constitute this group, however, as compared to
621 Jonkers and Kučera, (2015), we showed a strong and significant negative correlation of these two
622 species abundances with the SST (Figure 5). The latter work stated that the cycles of these species
623 were independent of the temperature changes, however, these two species tend to be used as
624 tracers of cool and deep mesotrophic waters in the Mediterranean, generally associated with the
625 MAW (Azibeiro et al., 2023).

626 In summary, our data showed that in the Sicily Strait, the three major ecological groups proposed
627 by Jonkers and Kučera, (2015), exhibited a different response to environmental variability. Overall,
628 groups 1 and 3 showed significant correlation with the latter parameters and were in accordance
629 with their corresponding species ecologies. However, group 2 did not show any significant
630 correlation, which we interpreted as the result of very low abundances of the taxa comprised within
631 this group. This translates into the dominance of group 1 during summer and autumn when



632 oligotrophic and warm eastern waters dominate the water column, while the mesotrophic taxa from
633 group 3 dominate during winter and spring, coincidentally with higher primary productivity, yet not
634 eutrophic enough for the opportunistic taxa comprised in the group 2, which is less well represented
635 in the Sicily Strait.
636



637
638 **Figure 5.** SST and chlorophyll-*a* concentration against the relative abundance of the five most abundant
639 species and the three ecological groups proposed by Jonkers and Kučera (2015). Orange dots stand for
640 SST while the green ones correspond to chlorophyll-*a*.
641

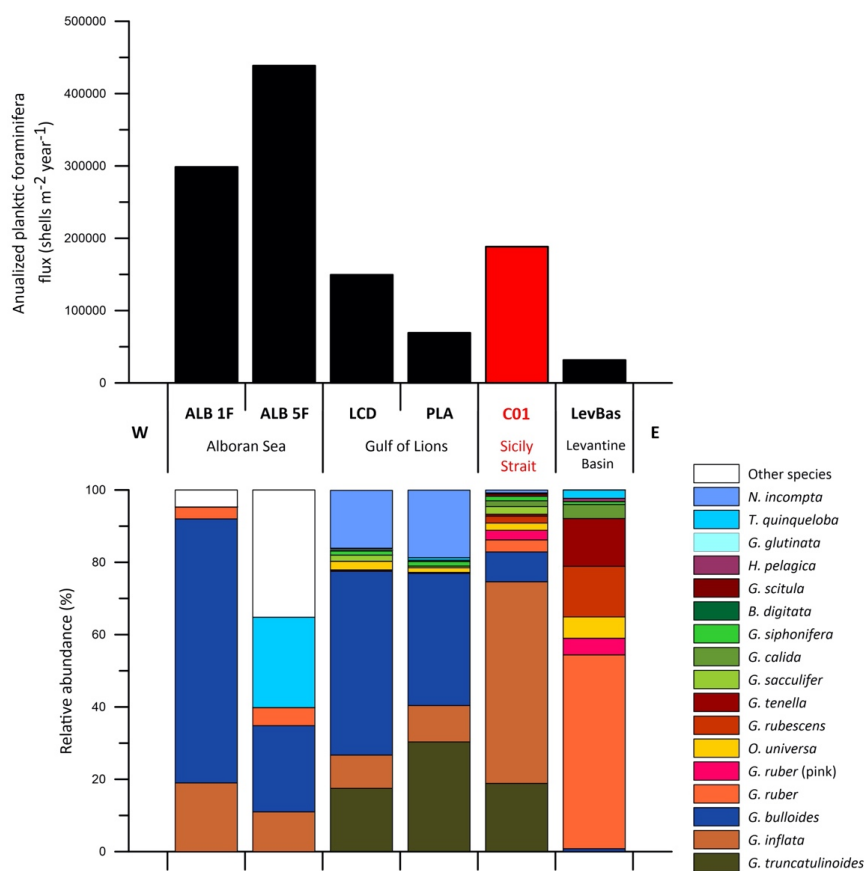
642 **5.3 Geographical variability in the magnitude and composition of planktic foraminifera fluxes** 643 **across the Mediterranean**

644 The comparison of the Sicily Strait planktic foraminifera sediment trap record with the ones
645 retrieved from different parts of the Mediterranean offers a unique opportunity to provide further
646 insight into the dynamics and ecology of this group on a basin-wide scale.

647 As stated previously, the planktic foraminifera flux in the Sicily Strait was higher from mid-January
648 to mid-March, which coincided with the highest chlorophyll concentrations and the coolest SST
649 recorded (Figure 2). This seasonality is similar to the one observed in the Gulf of Lions, where the
650 planktic foraminifera flux reached its highest values from mid-February to mid-March during
651 different years (Rigual-Hernández et al., 2012). Although slightly different, the planktic foraminifera
652 fluxes patterns from both the Levantine basin and the Alboran Sea also displayed maximum values
653 between mid-February to mid-March and mid-January to mid-February respectively (Avnaim-Katav
654 et al., 2020; Hernández-Almeida et al., 2011). However, the magnitude of the planktic foraminifera
655 flux values displayed some differences between the sites (see Supplementary Figure). Overall, for
656 the Sicily Strait, values ranged between 0-1889 shells m⁻² d⁻¹ with a mean value of 629 shells m⁻² d⁻¹.
657 These values were comparable to the ones from the Gulf of Lions: 0-2114 and 4268 shells m⁻² d⁻¹
658 with a mean value of 225.4 in Planier sediment trap to 419 shells m⁻² d⁻¹ in Lacaze-Duthiers sediment
659 trap. On the other hand, the Levantine basin values were lower: 0-429 shells m⁻² d⁻¹, with a mean
660 value of 93 shells m⁻² d⁻¹. Finally, the highest values belonged to the Alboran Sea: 0-6000 shells m⁻²



661 d^{-1} with a mean value of 783 to 970 shells $m^{-2} d^{-1}$ depending on the gyres. Note that the planktic
662 foraminifera flux values from the Levantine basin used here represent the foraminifera shells from
663 the $>125 \mu m$ fraction, which highlights the fact that compared to the $>150 \mu m$, the flux values
664 should be even lower. The corresponding chlorophyll-*a* values registered in the latter sites were 0.2-
665 0.65 $mg m^{-3}$ for the Sicily Strait (Figure 5), 0.25-0.85 $mg m^{-3}$ for the Gulf of Lions (0-0.65 $mg m^{-3}$ in
666 the Planier site, 0.25-0.85 $mg m^{-3}$ for Lacaze-Duthiers) (Rigual-Hernández et al., 2012), 0.02-0.4 mg
667 m^{-3} for the Levantine basin (Avnaim-Katav et al., 2020) and 0.1-1.2 $mg m^{-3}$ in the Alboran Sea
668 (Hernández-Almeida et al., 2011), indicating a similar productivity in terms of chlorophyll-*a* between
669 the Gulf of Lions and the Sicily Strait. In addition, here we calculated an annualized planktic
670 foraminifera flux (section 3.4) for each of the 6 sites compared here (Figure 6). Overall, the highest
671 annualized fluxes were displayed in the Alboran Sea (Figure 6): around 3×10^5 and 4.4×10^5 shells m^{-2}
672 y^{-1} , while the lowest one was displayed in the Levantine Basin: a little over 30000 shells $m^{-2} y^{-1}$ (Figure
673 6). The Gulf of Lions and the Sicily Strait displayed comparable annualized fluxes although higher for
674 the latter: around 1.5×10^5 and 1.85×10^5 shells $m^{-2} y^{-1}$ respectively. Note that PLA site values were
675 significantly lower: around 7×10^4 shells $m^{-2} y^{-1}$ (Figure 6). Previous work showed that these planktic
676 foraminifera patterns were mainly linked to specific regional oceanographic processes. First of all,
677 the Levantine basin is well known for being an ultra-oligotrophic region and being the warmest and
678 saltiest of the Mediterranean basins (Ozer et al., 2017), mainly due to the W-E anti-estuarine
679 circulation. On the other hand, the Gulf of Lions is considered an exception to the general
680 oligotrophy of the Mediterranean. Seasonal vertical mixing phenomenon occurs in winter,
681 generated by cold winds. This winter mixing recharges the surface waters with nutrients, allowing a
682 winter/spring productivity bloom (Durrieu de Madron et al., 2013; Houpert et al., 2016). Finally, the
683 Alboran Sea is a transitional region between the Atlantic Ocean and the Mediterranean Sea
684 (Hernández-Almeida et al., 2011), and unlike the latter, is not an oligotrophic region due to the two
685 systems of high productivity related to the gyres generated by an intense westerlies activity, which
686 allow nutrients enriched (compared to the resident waters) Atlantic waters to spread into the
687 Mediterranean. This results in an enhanced primary productivity period from November to March.
688 According to the PFF patterns displayed in this study, the Sicily Strait presents similar values and
689 fluxes distributions to the Gulf of Lions, however, its oceanographic circulation is significantly
690 different from the latter. These observations agree with the work of Mallo et al., (2017) carried out
691 with plankton tows in the whole Mediterranean basin. The latter work found that the Alboran Sea
692 displayed the highest standing stocks of planktic foraminifera, while the easternmost part of the
693 Mediterranean showed the minimum values. Also, the Gulf of Lions and the Strait of Sicily displayed
694 similar stocks, although slightly superior for the Strait of Sicily.



695
 696 **Figure 6.** Comparison of the annualized (see section 3....) planktic foraminifera flux and the relative
 697 abundance of each species identified in different time-series across the Mediterranean Sea (see section
 698 3...). The data from the Sicily Strait (C01) is depicted in red. Note that the Levantine Basin (LevBas)
 699 dataset covers the >125 μm fraction. Other species (white bar) in the Alboran Sea corresponds to any species
 700 different from the main 4 taxons identified in Bárcena et al., (2004) and Hernández-Almeida et al., (2011).
 701
 702 Concerning the species composition, we identified 15 planktic foraminifera species in the Sicily
 703 Strait, which is a similar species number to the one from the Gulf of Lions (14 species) and higher
 704 than in the Levantine basin (10 different species). The Sicily Strait site displayed the highest planktic
 705 foraminifera assemblage diversity among the three sites compared: a mean 1-D and S/W index of
 706 0.68 and 1.57 respectively. (Table 2). Interestingly, despite showing a similar number of different
 707 species, the Gulf of Lions displayed the lowest diversity values, especially for the PLA site: mean 1-
 708 D of 0.55 and mean H/W of 1.08, while the LCD site 1-D and h/w were 0.58 and 1.15 respectively.
 709 These observations highlight that, although the annualized planktic foraminifera flux was similar
 710 between the Gulf of Lions (for the LCD site) and the Sicily Strait (Figure 6), the assemblage in the
 711 latter site was significantly more diverse regarding species composition. The composition of the
 712 annual planktic foraminifera population of the different species showed some differences between



713 the sites compared here. In the Levantine basin, the majority of the planktic foraminifera population
714 consisted of surface symbiont bearing species such as *G. ruber*, *G. ruber* (pink), *G. rubescens*, *G.*
715 *tenella*, *O. universa*, which are well adapted to the ultra-oligotrophic conditions (Lombard et al.,
716 2011; Schiebel and Hemleben, 2017). The latter species represented 96% of the total planktic
717 foraminifera in the Levantine basin, while the same species in the Sicily Strait accounted for around
718 10% of the total individuals (Figure 6). Note that both *G. rubescens* and *G. tenella* are considered
719 small-sized species (Chernihovsky et al., 2023) and their adult size is often smaller than 150 μm , so
720 it is possible that some individuals of those species may not be recorded in our data. On the other
721 hand, in the Gulf of Lions, the four main species were *G. bulloides*, *N. incompta*, *G. inflata* and *G.*
722 *truncatulinooides*, which represented 88 to 95% of the total planktic foraminifera (Rigual-Hernández
723 et al., 2012). These species tend to be associated with eutrophic to mesotrophic environments
724 which coincides with the Gulf of Lions locally enhanced primary productivity conditions. In the Sicily
725 Strait, the same species accounted for 83% of the total individuals, and, except for *N. incompta*, the
726 remaining three species were also the most abundant in our samples.

727

728 **Table 2.** Inverse Simpson (1-H) and Shannon-Weiner indexes mean, standard deviation (“Stan. Dev.”)
729 and maximum values for the two Gulf of Lions sites (PLA and LCD), the Sicily Strait (C01, this study) and
730 the Levantine Basin (LevBas).

	Gulf of Lions		Sicily Strait	Levantine Basin
	LCD	PLA	C01	LevBas
Simpson 1-H				
Mean	0.581	0.553	0.681	0.615
Stan. Dev.	0.168	0.180	0.132	0.144
Max	0.802	0.781	0.872	0.804
Shannon H/W				
Mean	1.151	1.078	1.572	1.230
Stan. Dev.	0.359	0.375	0.398	0.316
Max	1.789	1.630	2.188	1.759

731

732 Considering the planktic foraminifera fluxes patterns, the species diversity and the planktic
733 foraminifera most abundant species from each of the three Mediterranean time-series with which
734 we compared our data, we interpret that, from a planktic foraminifera population point of view, the
735 Sicily Strait could be considered as a transition zone and a biological corridor between the western
736 and eastern basins.

737

738 Finally, to put our data into a global context, here we compare our dataset with planktic foraminifera
739 data from the same size fraction retrieved in the Gulf of Mexico, high latitudes North Atlantic and
740 gyres region of the North Atlantic Ocean. In the northern Gulf of Mexico, from 2008 to 2010, the
741 $>150 \mu\text{m}$ PFF was comprised between 0 and slightly over 800 shells $\text{m}^{-2} \text{d}^{-1}$, with a mean value of
742 around 250 shells $\text{m}^{-2} \text{d}^{-1}$ (Poore et al., 2013). A total of 12 species were identified, with *G.*
743 *truncatulinooides*, *G. ruber* (pink) and *N. dutertrei* as the most abundant species recorded. On the



744 other hand, in the North and high-latitudes Atlantic Ocean, Wolfteich (1994), showed that the PFF
745 oscillated between 0 and around 5000 shells $\text{m}^{-2} \text{d}^{-1}$ for a mean value of 800 shells $\text{m}^{-2} \text{d}^{-1}$, while *G.*
746 *bulloides* and *N. incompta* were the most abundant species. Although the latter work only focused
747 on the most abundant species, additional work has documented more than 20 species in the vicinity
748 of the North-Atlantic gyres (Salmon et al., 2015), but around only three to four in the high latitudes.
749 This highlights that, from a planktic foraminifera population point of view on a wider scale, the Sicily
750 Strait displayed a higher planktic foraminifera flux and species richness compared to the tropical to
751 subtropical Gulf of Mexico and to the high latitudes of the North Atlantic, but lower values compared
752 to the North Atlantic gyres region.
753

754 **5.4 Recent planktonic foraminifera assemblage comparison with seabed sediment**

755

756 The Mediterranean Sea is often referred to as a climate change hotspot and a “laboratory basin” where
757 many global environmental trends are amplified (Bethoux et al., 1999). In particular, ocean warming is
758 expected to exceed the global average (Hassoun et al., 2022, 2015; Lazzari et al., 2014) while it is
759 considered a specially sensitive zone of the ocean to acidification due to the fast turnover of its waters
760 and penetration of anthropogenic CO_2 (Bethoux et al., 1999; Schneider et al., 2007). One of the main
761 questions about planktic foraminifera concerns the way they are going to react to the ongoing climate
762 change in the global ocean (Jonkers and Kučera, 2015; Schiebel and Hemleben, 2017). Previous work
763 suggests that global communities of planktic foraminifera have already been affected by environmental
764 change since the onset of industrialization (Jonkers et al., 2019). Moreover, recent work has shown that
765 the calcification of several planktic foraminifera species has decreased during the industrial era in the
766 northwestern Mediterranean (Béjard et al., 2023). Therefore, here we aim to assess if modern planktonic
767 foraminifera communities dwelling in the Sicily Strait differ from their pre-industrial counterparts. To do
768 so, next, we compare the annual integrated assemblages collected by the C01 sediment trap with the
769 ones from a set of core-tops retrieved in the vicinity of the studied zone (see Section 3.5).

770 As planktic foraminifera are a group of calcifying plankton, when comparing sediment trap and
771 seabed sediment data, the possible role of calcite dissolution must be discussed. Firstly, the
772 Mediterranean Sea is supersaturated with respect to calcite (Álvarez et al., 2014; Millero et al., 1979)
773 and the depth of the studied material is substantially shallower than the calcite saturation horizon
774 (Álvarez et al., 2014). Secondly, recent work suggests that calcite experiences little to negligible
775 changes in the water column and burial in recent sediments (Béjard et al., 2023; Pallacks et al.,
776 2023). All this evidence suggests that dissolution played a negligible role in the preservation of
777 planktonic foraminifera preserved in the sediment record in the study region.

778 The core-tops with which the C01 sediment trap data is compared were part of the MARGO
779 database (see Section 3.4 for more details). Note that the MARGO sites 3735 to 3739 seabed
780 sediment was taken using a trigger-weight corer (Thunell, 1978). However, samples 3658, 3672 and
781 3673 were retrieved using a piston corer (Hayes et al., 2005). Generally, sampling with the trigger-
782 weight method is considered to retrieve less mixed and disturbed sediment than the piston or box
783 corer sampling methods (Skinner and McCave, 2003; Wu et al., 2020). Therefore, the foraminifera
784 assemblages from the core-tops may likely represent a mix of Holocene foraminifera assemblages
785 rather than exclusively modern assemblages. Although the lack of dating control makes it impossible



786 to determine the exact date of the core top assemblages, our data suggest that the composition of
 787 modern foraminifera assemblages in the Sicily Strait has changed between the late Holocene and
 788 the present day. The reasons of this change are uncertain, although we speculate that ongoing
 789 warming (Lazzari et al., 2014), the consequent increasing stratification of the water column in the
 790 Mediterranean (Siokou-Frangou et al., 2010) and a shift in the oceanographical configuration could
 791 have already reduced primary production in the Sicily Strait.

792
 793 **Table 3.** MARGO core-tops analyzed, their latitude and longitude and the squared chord distance (SCD)
 794 between the C01 sediment trap and the MARGO database core-tops. The complete SCD for all sites can
 795 be found in Supplementary data.

Site	MARGO database															
	3655	3677	3724	3739	3737	3738	3658	3725	3654	3680	3735	3736	3673	3727	3661	3726
Latitude	38.25	36.47	35.85	36.73	38.33	38.00	36.68	36.49	38.22	37.46	38.17	38.23	39.40	38.93	39.41	38.64
Longitude	13.35	11.49	13.03	13.95	11.80	11.78	12.28	13.32	13.27	11.55	11.23	11.25	13.34	10.59	13.34	10.78
SCD to C01	0.27	0.52	0.55	0.56	0.66	0.78	0.84	0.85	0.88	0.89	0.90	0.93	1.03	1.03	1.07	1.10

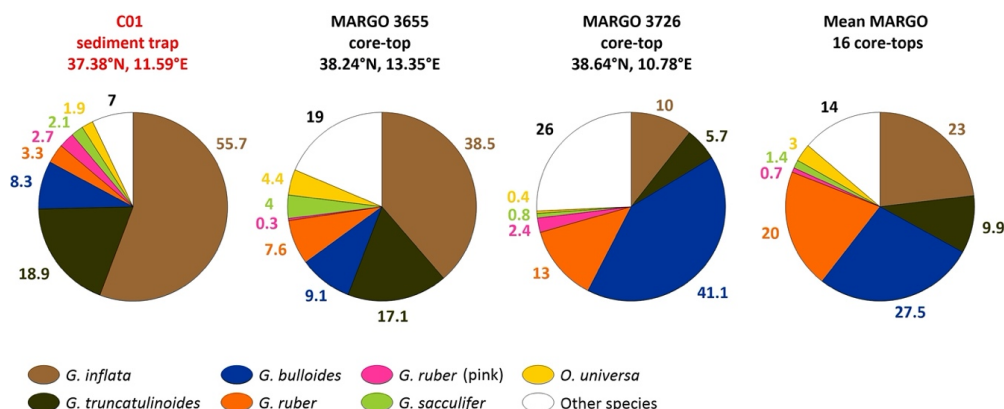
796
 797 The SCD between the annual integrated foraminifera assemblage of the C01 sediment trap and the
 798 core-tops from the Sicily Strait and adjacent areas (see Supplementary Figure 2) ranged between
 799 0.27 and 1.1 (Table 3). By using a dissimilarity coefficient value of <0.25 as cutoff criteria (see section
 800 3.4 for more details), it can be concluded that none of the core-tops assemblages can be considered
 801 close analogues to the C01 sediment trap. The only exception might be MARGO site 3655, located
 802 around 180 km northeast of the sediment trap, which displayed an SCD value of 0.27, very close to
 803 our cutoff threshold. The mean SCD between all core-tops and the sediment trap is 0.8, which
 804 contrasts with the SCD between the core-tops, which exhibited an average value between them of
 805 0.47 (see Supplementary data), indicating a higher similarity between them than with the sediment
 806 trap. Interestingly, from a geographical point of view, the geographical closest site analyzed
 807 (MARGO 3680) displayed a high SCD (0.89) despite being retrieved virtually in the underlying
 808 sediments beneath the C01 sediment trap (Table 3). Overall, the 4 most similar sites (SCD <0.6) to
 809 the sediment trap assemblage are all located eastward, while the 4 most different sites (SCD >1) are
 810 all located northward to the location of the sediment trap. This highlights the geographical
 811 variability of the Sicily Strait regarding the planktic foraminifera population and the complex
 812 oceanographic conditions. We speculate that the C01 sediment trap, in addition to registering
 813 species from both the western and eastern Mediterranean basins, could also be considered a key
 814 point in an east to west planktic foraminifera population gradient. Interestingly, the most different
 815 core-tops are located in the vicinity of the Tyrrhennian Sea and the most similar ones can be found
 816 in the easternmost part of the Sicily Strait. In combination with the dominant taxa registered, we
 817 propose that the MAW and western basin waters influence could have spread further east into the
 818 Sicily Strait. This, in combination with the resident eastern basin waters, could reconcile the planktic
 819 foraminifera assemblage described from the C01 sediment trap and the fact that it is more similar
 820 to core-tops located eastward.



821 In terms of planktic foraminifera assemblage composition, the most evident observation relies on
822 the shift of the dominant taxa when comparing the sediment trap and core-top assemblages (Figure
823 7). As described previously, *G. inflata* dominated the assemblages in the C01 sediment trap (Table
824 1), while *G. bulloides* is the best-represented species in the seabed sediment, followed by *G. inflata*
825 and *G. ruber* (Figure 7). The latter species showed mean relative abundances of 27.5%, 23% and 20%
826 across all core-tops, respectively. Interestingly, *G. truncatulinoides* abundance was significantly
827 lower in the core-tops while the “other species” category, which consists of minor taxa such as *G.*
828 *rubescens*, *G. siphonifera* and *G. calida* (amongst others) played a more significant role in the seabed
829 sediment, reaching abundances up to 26% (Figure 7). These results lead to several observations.
830 Firstly, *G. bulloides*, considered more susceptible to dissolution than the average planktic
831 foraminifera species (Dittert et al., 1999), dominates the seabed sediment assemblages; and *G.*
832 *inflata*, considered a less dissolution susceptible species (Schiebel and Hemleben, 2017) dominates
833 the sediment trap population. This information reinforces the idea that calcite dissolution in the
834 water column or sediments is negligible. In other words, if dissolution was to take place here, *G.*
835 *inflata* would be overrepresented in the seabed sediment, which is not the case. Secondly, the
836 seabed sediment planktic foraminifera populations showed a reduced influence of deep-dwelling
837 species and a more pronounced influence of both eutrophic and oligotrophic species. These
838 eutrophic species (such as *G. bulloides* but also *N. incompta*) are associated with MAW and western
839 basins in the modern Mediterranean Sea, while the more oligotrophic taxa (*G. ruber*, *G. rubescens*,
840 *G. calida*...) are considered to be transported from the easternmost part of the basin (Azibeiro et al.,
841 2023). A possible interpretation of these results is that the MAW influence into the basin may have
842 shifted, and instead of bringing rich and eutrophic waters that would allow the development of
843 opportunistic species, it nowadays brings more mesotrophic water masses that favour the
844 development of deep dwellers in the Sicily Strait. On the other hand, this could also lead to the
845 assumption of a reduced eastward and LIW influence in the present day as seen by the significantly
846 lower abundance of oligotrophic species in the C01 sediment trap. Also, a change in the
847 environmental conditions could lead to the increase of deep dwellers in substitution of eutrophic
848 species such as *G. bulloides*. As described previously, the Mediterranean Sea has already been
849 described as a climate change “hotspot”, therefore the already documented ocean warming and
850 the consequent stratification (Malanotte-Rizzoli et al., 2014; Siokou-Frangou et al., 2010) could have
851 led to unfavorable conditions for several taxa. A decrease in the primary production might have
852 caused a shift in the dominance of the opportunistic *G. bulloides* by *G. inflata*. As described
853 previously, *G. bulloides* shows a high affinity for high productivity environments, while deep
854 dwellers such as *G. inflata* and *G. truncatulinoides* tend to prefer mesotrophic and stratified waters.
855 In that sense, the recent warming and stratification of the Mediterranean could explain the recent
856 trend in the planktic foraminifera population registered by the C01 sediment trap. However, in that
857 case, species such as *G. ruber* and other oligotrophic species should be at least as much represented
858 as in the seabed sediment. Alternatively, this could imply a change in the intensity of the water
859 masses flowing, such as an increased mesotrophic MAW influence and a reduced oligotrophic LIW
860 influence.
861 Therefore, here we theorize that a combination of environmental change and a shift in the
862 oceanographic configuration could explain the differences in the planktic foraminifera population



863 between the modern C01 sediment trap population and the seabed assemblages. Overall, these
 864 results call for increasing the monitoring of planktic foraminifera populations and accentuating the
 865 comparisons between recent and seabed sediment assemblages in the Mediterranean to determine
 866 if the trends suggested by our data are the result of the recent environmental change.
 867
 868



869
 870
 871 **Figure 7.** Comparison of the relative abundance of the planktic foraminifera from the sediment trap and
 872 seabed sediment. C01 sediment trap is depicted in red (first from the left). MARGO site 3655 corresponds
 873 to the lowest squared chord distance and MARGO site 3726 to the highest one. The last figure represents
 874 the mean relative abundance of all core-tops included in this study (see Supplementary data).
 875

876 Conclusions

877
 878 The C01 mooring line, located on the axis of the Sicily Strait, provided the opportunity to document
 879 the planktic foraminifera population on an interannual scale. We analyzed 19 samples that covered
 880 the timespan between November 2013 and October 2014. A total of 3723 individuals and 15
 881 different species were identified. *G. inflata*, *G. truncatulinooides*, *G. bulloides*, *G. ruber* and *G. ruber*
 882 (pink) were the five most abundant species, representing 56, 19, 8, 3.5 and 3% of the total
 883 foraminifera. The remaining species represented less than 5% of the total individuals. Total planktic
 884 foraminifera flux ranged between 44 and 1890 shells $m^{-2} d^{-1}$, higher values were reached during
 885 spring while values were lower during summer. Our data indicates that the planktic foraminifera
 886 fluxes mainly reflect the oceanographic configuration of the Sicily Strait and its seasonal surface
 887 circulation variability. During winter and spring, a stronger eastward advection favours the MAW
 888 entrance in the Sicily Strait, allowing cool and nutrient enriched waters to enter the strait. This
 889 resulted in an increased planktic foraminifera flux and a higher presence of *G. inflata*, *G.*
 890 *truncatulinooides* or *G. bulloides*, which are taxa associated with the western basin. On the other
 891 hand, during summer, the eastward advection is reduced and the LIW dominates the water column,
 892 favorizing the increase of species associated with the eastern basin, such as *G. ruber*, and *G. ruber*
 893 (pink). Our correlation data with both SST and chlorophyll-*a* showed that *G. inflata* was associated



894 with cool and nutrient rich waters. In contrast, both *G. ruber* species were associated with warm
895 and oligotrophic waters, which agrees with their ecology. Surprisingly, no significant trends were
896 identified for either *G. truncatulinoides* or *G. bulloides*. The comparison with integrated annual data
897 from other sediment trap experiments conducted in in different regions of the Mediterranean basin,
898 our fluxes and diversity data indicated that the Sicily Strait can be considered a transitional zone in
899 regard to planktic foraminifera populations: annualized fluxes were lower compared to the
900 westernmost Alboran Sea, but higher than in the easternmost Levantine basin. However, the Sicily
901 Strait exhibited the highest diversity values across all the sites analyzed, highlighting the influence
902 of both the western and eastern basins. Finally, the planktic foraminifera assemblages from the
903 sediment trap were significantly different from the ones coming from the seabed located in the
904 vicinity of the mooring line. In the sediment trap, deep dwellers dominated the planktic foraminifera
905 population, while both eutrophic and oligotrophic taxa were more abundant in the seabed
906 sediment. We propose a combination of two factors to explain these differences such as recent
907 environmental change, most likely warming and consequent shallowing of mixed layer depths; and
908 a shift in the oceanographical conditions in the recent Central Mediterranean.

909
910 *Data availability.* All data used in this study are presented in the Supplement and are available online
911 at doi: 10.17632/tp4v6hm7dc.1 (Béjard et al., 2023).

912
913 *Supplement.* The supplement related to this article is available online at:

914
915 *Author contributions.* ASRH, FJS and TMB designed the study. JPT designed Fig. 1 and contributed to
916 planktic foraminifera identification and imaging. ASV and ILC provided the JERICO C01 sediment trap
917 samples and led the sample processing. TMB led the microscopy and image analysis, the
918 foraminifera study, statistical analysis and wrote the manuscript with feedback from all authors.

919
920 *Competing interests.* The contact author has declared that none of the authors has any competing
921 interests.

922
923 *Acknowledgements.* The authors would like to thank Aidan Hunter from the BAS (Cambridge) for
924 the statistical analysis inputs and Francesca Bulian (University of Groningen) for benthic
925 foraminifera identification support.

926
927 *Financial support.* This research has been supported by the Ministerio de Ciencia e Innovación (grant
928 nos. RTI2018-099489-B-100, PID2021-128322NB-100, and PRE2019-089091). This research has also
929 received funding from the JERICO project under the FP7 contract agreement nº 262584 and
930 supported by ISMAR, CNR. ASV acknowledges the financial support by the Catalan Government
931 Grups de Recerca Consolidats grant (2021 SGR 01195). This project has received funding from the
932 project BASELINE (grant no. PID2021- 126495NB-741 C33) granted by the Spanish Ministry of
933 Science and Innovation and Universities (Andrés S. Rigual-Hernández).

934
935 **References**



936

937 Aldridge, D., Beer, C. J., and Purdie, D. A.: Calcification in the planktonic foraminifera *Globigerina bulloides*; linked
938 to phosphate concentrations in surface waters of the North Atlantic Ocean, *Biogeosciences*, 9, 1725–1739,
939 <https://doi.org/10.5194/bg-9-1725-2012>, 2012.

940 Álvarez, M., Sanleón-Bartolomé, H., Tanhua, T., Mintrop, L., Luchetta, A., Cantoni, C., Schroeder, K., and Civitarese,
941 G.: The CO₂ system in the Mediterranean Sea: a basin wide perspective, *Ocean Sci.*, 10, 69–92,
942 <https://doi.org/10.5194/os-10-69-2014>, 2014.

943 Astraldi, M., Gasparini, G. P., Gervasio, L., and Salusti, E.: Dense Water Dynamics along the Strait of Sicily
944 (Mediterranean Sea), *J. Phys. Oceanogr.*, 31, 3457–3475, [https://doi.org/10.1175/1520-9450485\(2001\)031<3457:DWDATS>2.0.CO;2](https://doi.org/10.1175/1520-9450485(2001)031<3457:DWDATS>2.0.CO;2), 2001.

946 Astraldi, M., Gasparini, G. P., Vetrano, A., and Vignudelli, S.: Hydrographic characteristics and interannual
947 variability of water masses in the central Mediterranean: a sensitivity test for long-term changes in the
948 Mediterranean Sea, *Deep Sea Research Part I: Oceanographic Research Papers*, 49, 661–680,
949 [https://doi.org/10.1016/S0967-0637\(01\)00059-0](https://doi.org/10.1016/S0967-0637(01)00059-0), 2002.

950 Avnaim-Katav, S., Herut, B., Rahav, E., Katz, T., Weinstein, Y., Alkalay, R., Berman-Frank, I., Zlatkin, O., and Almogi-
951 Labin, A.: Sediment trap and deep sea coretop sediments as tracers of recent changes in planktonic
952 foraminifera assemblages in the southeastern ultra-oligotrophic Levantine Basin, *Deep Sea Research Part II:
953 Topical Studies in Oceanography*, 171, 104669, <https://doi.org/10.1016/j.dsr2.2019.104669>, 2020.

954 Azibeiro, L. A., Kučera, M., Jonkers, L., Cloke-Hayes, A., and Sierro, F. J.: Nutrients and hydrography explain the
955 composition of recent Mediterranean planktonic foraminiferal assemblages, *Marine Micropaleontology*, 179,
956 102201, <https://doi.org/10.1016/j.marmicro.2022.102201>, 2023.

957 Balestra, B., Grunert, P., Ausin, B., Hodell, D., Flores, J.-A., Alvarez-Zarikian, C. A., Hernandez-Molina, F. J., Stow, D.,
958 Piller, W. E., and Paytan, A.: Coccolithophore and benthic foraminifera distribution patterns in the Gulf of
959 Cadiz and Western Iberian Margin during Integrated Ocean Drilling Program (IODP) Expedition 339, *Journal of
960 Marine Systems*, 170, 50–67, <https://doi.org/10.1016/j.jmarsys.2017.01.005>, 2017.

961 Bárcena, M. A., Flores, J. A., Sierro, F. J., Pérez-Folgado, M., Fabres, J., Calafat, A., and Canals, M.: Planktonic
962 response to main oceanographic changes in the Alboran Sea (Western Mediterranean) as documented in
963 sediment traps and surface sediments, *Marine Micropaleontology*, 53, 423–445,
964 <https://doi.org/10.1016/j.marmicro.2004.09.009>, 2004.

965 Barker, S. and Elderfield, H.: Foraminiferal Calcification Response to Glacial-Interglacial Changes in Atmospheric
966 CO₂, *Science*, 297, 833–836, <https://doi.org/10.1126/science.1072815>, 2002.

967 Bé, A. W. H., Hutson, W. H., and Be, A. W. H.: Ecology of Planktonic Foraminifera and Biogeographic Patterns of
968 Life and Fossil Assemblages in the Indian Ocean, *Micropaleontology*, 23, 369,
969 <https://doi.org/10.2307/1485406>, 1977.

970 Beer, C. J., Schiebel, R., and Wilson, P. A.: Testing planktic foraminiferal shell weight as a surface water [CO₃–]
971 proxy using plankton net samples, *Geology*, 38, 103–106, <https://doi.org/10.1130/G30150.1>, 2010.

972 Béjard, T. M., Rigual-Hernández, A. S., Flores, J. A., Tarruella, J. P., Durrieu De Madron, X., Cacho, I., Haghpor, N.,
973 Hunter, A., and Sierro, F. J.: Calcification response of planktic foraminifera to environmental change in the
974 western Mediterranean Sea during the industrial era, *Biogeosciences*, 20, 1505–1528,
975 <https://doi.org/10.5194/bg-20-1505-2023>, 2023.

976 Béranger, K., Mortier, L., Gasparini, G.-P., Gervasio, L., Astraldi, M., and Crépon, M.: The dynamics of the Sicily
977 Strait: a comprehensive study from observations and models, *Deep Sea Research Part II: Topical Studies in
978 Oceanography*, 51, 411–440, <https://doi.org/10.1016/j.dsr2.2003.08.004>, 2004.

979 Bergamasco, A. and Malanotte-Rizzoli, P.: The circulation of the Mediterranean Sea: a historical review of
980 experimental investigations, *Advances in Oceanography and Limnology*, 1, 11–28,
981 <https://doi.org/10.1080/19475721.2010.491656>, 2010.

982 Bethoux, J. P., Gentili, B., Morin, P., Nicolas, E., Pierre, C., and Ruiz-Pino, D.: The Mediterranean Sea: a miniature
983 ocean for climatic and environmental studies and a key for the climatic functioning of the North Atlantic,
984 *Progress in Oceanography*, 44, 131–146, [https://doi.org/10.1016/S0079-6611\(99\)00023-3](https://doi.org/10.1016/S0079-6611(99)00023-3), 1999.

985 Bijma, J., Faber, W. W., and Hemleben, C.: Temperature and salinity limits for growth and survival of some
986 planktonic foraminifers in laboratory cultures, *The Journal of Foraminiferal Research*, 20, 95–116,
987 <https://doi.org/10.2113/gsjfr.20.2.95>, 1990.



- 988Bijma, J., Hönisch, B., and Zeebe, R. E.: Impact of the ocean carbonate chemistry on living foraminiferal shell weight:
989 Comment on “Carbonate ion concentration in glacial-age deep waters of the Caribbean Sea” by W. S. Broecker
990 and E. Clark: COMMENT, *Geochem.-Geophys.-Geosyst.*, 3, 1–7, <https://doi.org/10.1029/2002GC000388>,
991 2002.
- 992Bouzinac, C., Font, J., and Millot, C.: Hydrology and currents observed in the channel of Sardinia during the PRIMO-
993 1 experiment from November 1993 to October 1994, *Journal of Marine Systems*, 20, 333–355,
994 [https://doi.org/10.1016/S0924-7963\(98\)00074-8](https://doi.org/10.1016/S0924-7963(98)00074-8), 1999.
- 995Chapman, M. R.: Seasonal production patterns of planktonic foraminifera in the NE Atlantic Ocean: Implications
996 for paleotemperature and hydrographic reconstructions: CURRENTS, *Paleoceanography*, 25,
997 <https://doi.org/10.1029/2008PA001708>, 2010.
- 998Chernihovsky, N., Torfstein, A., and Almogi-Labin, A.: Seasonal flux patterns of planktonic foraminifera in a deep,
999 oligotrophic, marginal sea: Sediment trap time series from the Gulf of Aqaba, northern Red Sea, *Deep Sea*
1000 *Research Part I: Oceanographic Research Papers*, 140, 78–94, <https://doi.org/10.1016/j.dsr.2018.08.003>,
1001 2018.
- 1002Chernihovsky, N., Torfstein, A., and Almogi-Labin, A.: Daily timescale dynamics of planktonic foraminifera shell-size
1003 distributions, *Front. Mar. Sci.*, 10, 1126398, <https://doi.org/10.3389/fmars.2023.1126398>, 2023.
- 1004Cisneros, M., Cacho, I., Frigola, J., Canals, M., Masqué, P., Martrat, B., Casado, M., Grimalt, J. O., Pena, L. D.,
1005 Margaritelli, G., and Lirer, F.: Sea surface temperature variability in the central-western Mediterranean Sea
1006 during the last 2700 years: a multi-proxy and multi-record approach, *Clim. Past*, 12, 849–869,
1007 <https://doi.org/10.5194/cp-12-849-2016>, 2016.
- 1008Dittert, N., Baumann, K.-H., Bickert, T., Henrich, R., Huber, R., Kinkel, H., and Meggers, H.: Carbonate Dissolution
1009 in the Deep-Sea: Methods, Quantification and Paleoceanographic Application, in: *Use of Proxies in*
1010 *Paleoceanography*, edited by: Fischer, G. and Wefer, G., Springer Berlin Heidelberg, Berlin, Heidelberg, 255–
1011 284, https://doi.org/10.1007/978-3-642-58646-0_10, 1999.
- 1012D’Ortenzio, F.: On the trophic regimes of the Mediterranean Sea: a satellite analysis, 2009.
- 1013Ducassou, E., Hassan, R., Gonthier, E., Duprat, J., Hanquiez, V., and Mulder, T.: Biostratigraphy of the last 50 kyr in
1014 the contourite depositional system of the Gulf of Cádiz, *Marine Geology*, 395, 285–300,
1015 <https://doi.org/10.1016/j.margeo.2017.09.014>, 2018.
- 1016Durrieu de Madron, X., Houpert, L., Puig, P., Sanchez-Vidal, A., Testor, P., Bosse, A., Estournel, C., Somot, S.,
1017 Bourrin, F., Bouin, M. N., Beauverger, M., Beguery, L., Calafat, A., Canals, M., Cassou, C., Coppola, L., Dausse,
1018 D., D’Ortenzio, F., Font, J., Heussner, S., Kunesch, S., Lefevre, D., Le Goff, H., Martín, J., Mortier, L., Palanques,
1019 A., and Raimbault, P.: Interaction of dense shelf water cascading and open-sea convection in the northwestern
1020 Mediterranean during winter 2012: SHELF CASCADING AND OPEN-SEA CONVECTION, *Geophys. Res. Lett.*, 40,
1021 1379–1385, <https://doi.org/10.1002/grl.50331>, 2013.
- 1022Fox, L., Stukins, S., Hill, T., and Miller, C. G.: Quantifying the Effect of Anthropogenic Climate Change on Calcifying
1023 Plankton, *Sci Rep*, 10, 1620, <https://doi.org/10.1038/s41598-020-58501-w>, 2020.
- 1024Gasparini, G. P., Ortona, A., Budillon, G., Astraldi, M., and Sansone, E.: The effect of the Eastern Mediterranean
1025 Transient on the hydrographic characteristics in the Strait of Sicily and in the Tyrrhenian Sea, *Deep Sea*
1026 *Research Part I: Oceanographic Research Papers*, 52, 915–935, <https://doi.org/10.1016/j.dsr.2005.01.001>,
1027 2005.
- 1028Gaudy, R., Youssara, F., Diaz, F., and Raimbault, P.: Biomass, metabolism and nutrition of zooplankton in the Gulf
1029 of Lions (NW Mediterranean), *Oceanologica Acta*, 26, 357–372, [https://doi.org/10.1016/S0399-1030-1784\(03\)00016-1](https://doi.org/10.1016/S0399-1030-1784(03)00016-1), 2003.
- 1031Hassoun, A. E. R., Gemayel, E., Krasakopoulou, E., Goyet, C., Abboud-Abi Saab, M., Guglielmi, V., Touratier, F., and
1032 Falco, C.: Acidification of the Mediterranean Sea from anthropogenic carbon penetration, *Deep Sea Research*
1033 *Part I: Oceanographic Research Papers*, 102, 1–15, <https://doi.org/10.1016/j.dsr.2015.04.005>, 2015.
- 1034Hassoun, A. E. R., Bantelman, A., Canu, D., Comeau, S., Galdies, C., Gattuso, J.-P., Giani, M., Grelaud, M., Hendriks,
1035 I. E., Ibello, V., Idrissi, M., Krasakopoulou, E., Shaltout, N., Solidoro, C., Swarzenski, P. W., and Ziveri, P.: Ocean
1036 acidification research in the Mediterranean Sea: Status, trends and next steps, *Front. Mar. Sci.*, 9, 892670,
1037 <https://doi.org/10.3389/fmars.2022.892670>, 2022.
- 1038Hayes, A., Kucera, M., Kallel, N., Sbaffi, L., and Rohling, E. J.: Compilation of planktic foraminifera modern data from
1039 the Mediterranean Sea, <https://doi.org/10.1594/PANGAEA.227305>, 2005.



- 1040 Hazan, O., Silverman, J., Sisma-Ventura, G., Ozer, T., Gertman, I., Shoham-Frider, E., Kress, N., and Rahav, E.:
1041 Mesopelagic Prokaryotes Alter Surface Phytoplankton Production during Simulated Deep Mixing Experiments
1042 in Eastern Mediterranean Sea Waters, *Front. Mar. Sci.*, 5, 1, <https://doi.org/10.3389/fmars.2018.00001>, 2018.
- 1043 Hemleben, C., Spindler, M., and Anderson, O. R.: Modern Planktonic Foraminifera, 1989.
- 1044 Hernández-Almeida, I., Bárcena, M. A., Flores, J. A., Sierro, F. J., Sanchez-Vidal, A., and Calafat, A.: Microplankton
1045 response to environmental conditions in the Alboran Sea (Western Mediterranean): One year sediment trap
1046 record, *Marine Micropaleontology*, 78, 14–24, <https://doi.org/10.1016/j.marmicro.2010.09.005>, 2011.
- 1047 Heussner, S., Ratti, C., and Carbonne, J.: The PPS 3 time-series sediment trap and the trap sample processing
1048 techniques used during the ECOMARGE experiment, *Continental Shelf Research*, 10, 943–958,
1049 [https://doi.org/10.1016/0278-4343\(90\)90069-X](https://doi.org/10.1016/0278-4343(90)90069-X), 1990.
- 1050 Heussner, S., Durrieu de Madron, X., Calafat, A., Canals, M., Carbonne, J., Delsaut, N., and Saragoni, G.: Spatial and
1051 temporal variability of downward particle fluxes on a continental slope: Lessons from an 8-yr experiment in
1052 the Gulf of Lions (NW Mediterranean), *Marine Geology*, 234, 63–92,
1053 <https://doi.org/10.1016/j.margeo.2006.09.003>, 2006.
- 1054 Houpert, L., Durrieu de Madron, X., Testor, P., Bosse, A., D’Ortenzio, F., Bouin, M. N., Dausse, D., Le Goff, H.,
1055 Kunesch, S., Labaste, M., Coppola, L., Mortier, L., and Raimbault, P.: Observations of open-ocean deep
1056 convection in the northwestern Mediterranean Sea: Seasonal and interannual variability of mixing and deep
1057 water masses for the 2007-2013 Period: DEEP CONVECTION OBS. NWMED 2007-2013, *J. Geophys. Res.*
1058 *Oceans*, 121, 8139–8171, <https://doi.org/10.1002/2016JC011857>, 2016.
- 1059 Huertas, I. E., Ríos, A. F., García-Lafuente, J., Navarro, G., Makaoui, A., Sánchez-Román, A., Rodríguez-Galvez, S.,
1060 Orbi, A., Ruíz, J., and Pérez, F. F.: Atlantic forcing of the Mediterranean oligotrophy: ATLANTIC FORCING OF
1061 MEDITERRANEAN OLIGOTROPHY, *Global Biogeochem. Cycles*, 26, n/a-n/a,
1062 <https://doi.org/10.1029/2011GB004167>, 2012.
- 1063 Incarbona, A., Sprovieri, M., Lirer, F., and Sprovieri, R.: Surface and deep water conditions in the Sicily channel
1064 (central Mediterranean) at the time of sapropel S5 deposition, *Palaeogeography, Palaeoclimatology,*
1065 *Palaeoecology*, 306, 243–248, <https://doi.org/10.1016/j.palaeo.2011.04.030>, 2011.
- 1066 Jonkers, L. and Kučera, M.: Global analysis of seasonality in the shell flux of extant planktonic Foraminifera,
1067 *Biogeosciences*, 12, 2207–2226, <https://doi.org/10.5194/bg-12-2207-2015>, 2015.
- 1068 Jonkers, L., Hillebrand, H., and Kucera, M.: Global change drives modern plankton communities away from the pre-
1069 industrial state, *Nature*, 570, 372–375, <https://doi.org/10.1038/s41586-019-1230-3>, 2019.
- 1070 Jouini, M., Béranger, K., Arsouze, T., Beuvier, J., Thiria, S., Crépon, M., and Taupier-Letage, I.: The Sicily Channel
1071 surface circulation revisited using a neural clustering analysis of a high-resolution simulation, *JGR Oceans*, 121,
1072 4545–4567, <https://doi.org/10.1002/2015JC011472>, 2016.
- 1073 Kemle-von Mücke, S. and Oberhänsli, H.: The Distribution of Living Planktic Foraminifera in Relation to Southeast
1074 Atlantic Oceanography, in: *Use of Proxies in Paleooceanography*, edited by: Fischer, G. and Wefer, G., Springer
1075 Berlin Heidelberg, Berlin, Heidelberg, 91–115, https://doi.org/10.1007/978-3-642-58646-0_3, 1999.
- 1076 Kiss, P., Jonkers, L., Hudáčková, N., Reuter, R. T., Donner, B., Fischer, G., and Kucera, M.: Determinants of Planktonic
1077 Foraminifera Calcite Flux: Implications for the Prediction of Intra- and Inter-Annual Pelagic Carbonate Budgets,
1078 *Global Biogeochem. Cycles*, 35, <https://doi.org/10.1029/2020GB006748>, 2021.
- 1079 Kroeker, K. J., Kordas, R. L., Crim, R., Hendriks, I. E., Ramajo, L., Singh, G. S., Duarte, C. M., and Gattuso, J.: Impacts
1080 of ocean acidification on marine organisms: quantifying sensitivities and interaction with warming, *Glob*
1081 *Change Biol*, 19, 1884–1896, <https://doi.org/10.1111/gcb.12179>, 2013.
- 1082 Krom, M. D., Kress, N., Brenner, S., and Gordon, L. I.: Phosphorus limitation of primary productivity in the eastern
1083 Mediterranean Sea, *Limnol. Oceanogr.*, 36, 424–432, <https://doi.org/10.4319/lo.1991.36.3.0424>, 1991.
- 1084 Krom, M. D., Woodward, E. M. S., Herut, B., Kress, N., Carbo, P., Mantoura, R. F. C., Spyres, G., Thingstad, T. F.,
1085 Wassmann, P., Wexels-Riser, C., Kitidis, V., Law, C. S., and Zodiatis, G.: Nutrient cycling in the south east
1086 Levantine basin of the eastern Mediterranean: Results from a phosphorus starved system, *Deep Sea Research*
1087 *Part II: Topical Studies in Oceanography*, 52, 2879–2896, <https://doi.org/10.1016/j.dsr2.2005.08.009>, 2005.
- 1088 Kuroyanagi, A. and Kawahata, H.: Vertical distribution of living planktonic foraminifera in the seas around Japan,
1089 *Marine Micropaleontology*, 53, 173–196, <https://doi.org/10.1016/j.marmicro.2004.06.001>, 2004.
- 1090 Lazzari, P., Mattia, G., Solidoro, C., Salon, S., Crise, A., Zavatarelli, M., Oddo, P., and Vichi, M.: The impacts of climate
1091 change and environmental management policies on the trophic regimes in the Mediterranean Sea: Scenario
1092 analyses, *Journal of Marine Systems*, 135, 137–149, <https://doi.org/10.1016/j.jmarsys.2013.06.005>, 2014.



- 1093 Lermusiaux, P. F. J. and Robinson, A. R.: Features of dominant mesoscale variability, circulation patterns and
1094 dynamics in the Strait of Sicily, Deep Sea Research Part I: Oceanographic Research Papers, 48, 1953–1997,
1095 [https://doi.org/10.1016/S0967-0637\(00\)00114-X](https://doi.org/10.1016/S0967-0637(00)00114-X), 2001.
- 1096 Lirer, F., Sprovieri, M., Vallefucio, M., Ferraro, L., Pelosi, N., Giordano, L., and Capotondi, L.: Planktonic
1097 foraminifera as bio-indicators for monitoring the climatic changes that have occurred over the past 2000 years
1098 in the southeastern Tyrrhenian Sea, Integrative Zoology, 9, 542–554, <https://doi.org/10.1111/1749-1099-4877.12083>, 2014.
- 1100 Lombard, F., Erez, J., Michel, E., and Labeyrie, L.: Temperature effect on respiration and photosynthesis of the
1101 symbiont-bearing planktonic foraminifera *Globigerinoides ruber*, *Orbulina universa*, and *Globigerinella*
1102 *siphonifera*, Limnol. Oceanogr., 54, 210–218, <https://doi.org/10.4319/lo.2009.54.1.0210>, 2009.
- 1103 Lombard, F., Labeyrie, L., Michel, E., Bopp, L., Cortijo, E., Retailleau, S., Howa, H., and Jorissen, F.: Modelling
1104 planktic foraminifer growth and distribution using an ecophysiological multi-species approach,
1105 Biogeosciences, 8, 853–873, <https://doi.org/10.5194/bg-8-853-2011>, 2011.
- 1106 Macias, D., Cózar, A., Garcia-Gorriz, E., González-Fernández, D., and Stips, A.: Surface water circulation develops
1107 seasonally changing patterns of floating litter accumulation in the Mediterranean Sea. A modelling approach,
1108 Marine Pollution Bulletin, 149, 110619, <https://doi.org/10.1016/j.marpolbul.2019.110619>, 2019.
- 1109 Malanotte-Rizzoli, P., Artale, V., Borzelli-Eusebi, G. L., Brenner, S., Crise, A., Gacic, M., Kress, N., Marullo, S., Ribera
1110 d'Alcalà, M., Sofianos, S., Tanhua, T., Theocharis, A., Alvarez, M., Ashkenazy, Y., Bergamasco, A., Cardin, V.,
1111 Carniel, S., Civitarese, G., D'Ortenzio, F., Font, J., Garcia-Ladona, E., Garcia-Lafuente, J. M., Gogou, A., Gregoire,
1112 M., Hainbucher, D., Kontoyannis, H., Kovacevic, V., Kraskapoulou, E., Kroskos, G., Incarbona, A., Mazzocchi,
1113 M. G., Orlic, M., Ozsoy, E., Pascual, A., Poulain, P.-M., Roether, W., Rubino, A., Schroeder, K., Siokou-Frangou,
1114 J., Souvermezoglou, E., Sprovieri, M., Tintoré, J., and Triantafyllou, G.: Physical forcing and
1115 physical/biochemical variability of the Mediterranean Sea: a review of unresolved issues and directions for
1116 future research, Ocean Sci., 10, 281–322, <https://doi.org/10.5194/os-10-281-2014>, 2014.
- 1117 Mallo, M., Ziveri, P., Mortyn, P. G., Schiebel, R., and Grelaud, M.: Low planktic foraminiferal diversity and
1118 abundance observed in a spring 2013 west–east Mediterranean Sea plankton tow transect, Biogeosciences,
1119 14, 2245–2266, <https://doi.org/10.5194/bg-14-2245-2017>, 2017.
- 1120 Margaritelli, G., Lirer, F., Schroeder, K., Alberico, I., Dentici, M. P., and Caruso, A.: Globorotalia truncatulinoides in
1121 Central - Western Mediterranean Sea during the Little Ice Age, Marine Micropaleontology, 161, 101921,
1122 <https://doi.org/10.1016/j.marmicro.2020.101921>, 2020.
- 1123 Margaritelli, G., Lirer, F., Schroeder, K., Cloke-Hayes, A., Caruso, A., Capotondi, L., Broggy, T., Cacho, I., and Sierro,
1124 F. J.: Globorotalia truncatulinoides in the Mediterranean Basin during the Middle–Late Holocene: Bio-
1125 Chronological and Oceanographic Indicator, Geosciences, 12, 244,
1126 <https://doi.org/10.3390/geosciences12060244>, 2022.
- 1127 Marshall, B. J., Thunell, R. C., Henehan, M. J., Astor, Y., and Wejnert, K. E.: Planktonic foraminiferal area density as
1128 a proxy for carbonate ion concentration: A calibration study using the Cariaco Basin ocean time series:
1129 FORAMINIFERAL AREA DENSITY [CO₃²⁻] PROXY, Paleoceanography, 28, 363–376,
1130 <https://doi.org/10.1002/palo.20034>, 2013.
- 1131 Milker, Y. and Schmiedl, G.: A taxonomic guide to modern benthic shelf foraminifera of the western Mediterranean
1132 Sea, Palaeontologia Electronica, <https://doi.org/10.26879/271>, 2012.
- 1133 Millot, C.: Mesoscale and seasonal variabilities of the circulation in the western Mediterranean, Dynamics of
1134 Atmospheres and Oceans, 15, 179–214, [https://doi.org/10.1016/0377-0265\(91\)90020-G](https://doi.org/10.1016/0377-0265(91)90020-G), 1991.
- 1135 Millot, C.: Circulation in the Western Mediterranean Sea, Journal of Marine Systems, 20, 423–442,
1136 [https://doi.org/10.1016/S0924-7963\(98\)00078-5](https://doi.org/10.1016/S0924-7963(98)00078-5), 1999.
- 1137 Millot, C. and Taupier-Letage, I.: Circulation in the Mediterranean Sea, in: The Mediterranean Sea, vol. 5K, edited
1138 by: Saliot, A., Springer Berlin Heidelberg, Berlin, Heidelberg, 29–66, <https://doi.org/10.1007/b107143>, 2005.
- 1139 de Moel, H., Ganssen, G. M., Peeters, F. J. C., Jung, S. J. A., Kroon, D., Brummer, G. J. A., and Zeebe, R. E.: Planktic
1140 foraminiferal shell thinning in the Arabian Sea due to anthropogenic ocean acidification?, Biogeosciences, 6,
1141 1917–1925, <https://doi.org/10.5194/bg-6-1917-2009>, 2009.
- 1142 Morán, X. and Estrada, M.: Short-term variability of photosynthetic parameters and particulate and dissolved
1143 primary production in the Alboran Sea (SW Mediterranean), Mar. Ecol. Prog. Ser., 212, 53–67,
1144 <https://doi.org/10.3354/meps212053>, 2001.



- 1145Moy, A. D., Howard, W. R., Bray, S. G., and Trull, T. W.: Reduced calcification in modern Southern Ocean planktonic
1146 foraminifera, *Nature Geosci*, 2, 276–280, <https://doi.org/10.1038/ngeo460>, 2009.
- 1147Navarro, G., Almaraz, P., Caballero, I., Vázquez, Á., and Huertas, I. E.: Reproduction of Spatio-Temporal Patterns of
1148 Major Mediterranean Phytoplankton Groups from Remote Sensing OC-CCI Data, *Front. Mar. Sci.*, 4, 246,
1149 <https://doi.org/10.3389/fmars.2017.00246>, 2017.
- 1150Nielsen, S. N.: Numerical Ecology. Legendre P. and Legendre L., second ed., Elsevier, Amsterdam, p. 853, 1998.,
1151 *Ecological Modelling*, 132, 303–304, [https://doi.org/10.1016/S0304-3800\(00\)00291-X](https://doi.org/10.1016/S0304-3800(00)00291-X), 2000.
- 1152Ortiz, J. D. and Mix, A. C.: Comparison of Imbrie-Kipp Transfer Function and modern analog temperature estimates
1153 using sediment trap and core top foraminiferal faunas, *Paleoceanography*, 12, 175–190,
1154 <https://doi.org/10.1029/96PA02878>, 1997.
- 1155Osborne, E. B., Thunell, R. C., Marshall, B. J., Holm, J. A., Tappa, E. J., Benitez-Nelson, C., Cai, W., and Chen, B.:
1156 Calcification of the planktonic foraminifera *Globigerina bulloides* and carbonate ion concentration: Results
1157 from the Santa Barbara Basin, *Paleoceanography*, 31, 1083–1102, <https://doi.org/10.1002/2016PA002933>,
1158 2016.
- 1159Ozer, T., Gertman, I., Kress, N., Silverman, J., and Herut, B.: Interannual thermohaline (1979–2014) and nutrient
1160 (2002–2014) dynamics in the Levantine surface and intermediate water masses, SE Mediterranean Sea, *Global*
1161 *and Planetary Change*, 151, 60–67, <https://doi.org/10.1016/j.gloplacha.2016.04.001>, 2017.
- 1162Pallacks, S., Ziveri, P., Schiebel, R., Vonhof, H., Rae, J. W. B., Littley, E., Garcia-Orellana, J., Langer, G., Grelaud, M.,
1163 and Martrat, B.: Anthropogenic acidification of surface waters drives decreased biogenic calcification in the
1164 Mediterranean Sea, *Commun Earth Environ*, 4, 301, <https://doi.org/10.1038/s43247-023-00947-7>, 2023.
- 1165Poore, R. Z., Tedesco, K. A., and Spear, J. W.: Seasonal Flux and Assemblage Composition of Planktic Foraminifers
1166 from a Sediment-Trap Study in the Northern Gulf of Mexico, *Journal of Coastal Research*, 63, 6–19,
1167 <https://doi.org/10.2112/SI63-002.1>, 2013.
- 1168Prell, W. The Stability of Low-Latitude Sea-Surface Temperatures, an Evaluation of the CLIMAP Reconstruction with
1169 Emphasis on the Positive SST Anomalies. *Report No. TR025* (US Department of Energy), 1985.
- 1170Pujol, C. and Grazzini, C. V.: Distribution patterns of live planktic foraminifers as related to regional hydrography
1171 and productive systems of the Mediterranean Sea, *Marine Micropaleontology*, 25, 187–217,
1172 [https://doi.org/10.1016/0377-8398\(95\)00002-1](https://doi.org/10.1016/0377-8398(95)00002-1), 1995.
- 1173Raimbault, P., Pouvesle, W., Diaz, F., Garcia, N., and Sempéré, R.: Wet-oxidation and automated colorimetry for
1174 simultaneous determination of organic carbon, nitrogen and phosphorus dissolved in seawater, *Marine*
1175 *Chemistry*, 66, 161–169, [https://doi.org/10.1016/S0304-4203\(99\)00038-9](https://doi.org/10.1016/S0304-4203(99)00038-9), 1999.
- 1176Rebotim, A., Voelker, A. H. L., Jonkers, L., Waniek, J. J., Meggers, H., Schiebel, R., Fraile, I., Schulz, M., and Kucera,
1177 M.: Factors controlling the depth habitat of planktonic foraminifera in the subtropical eastern North Atlantic,
1178 *Biogeosciences*, 14, 827–859, <https://doi.org/10.5194/bg-14-827-2017>, 2017.
- 1179Rembauville, M., Meilland, J., Ziveri, P., Schiebel, R., Blain, S., and Salter, I.: Planktic foraminifer and coccolith
1180 contribution to carbonate export fluxes over the central Kerguelen Plateau, *Deep Sea Research Part I: Oceanographic*
1181 *Research Papers*, 111, 91–101, <https://doi.org/10.1016/j.dsr.2016.02.017>, 2016.
- 1182Retailleau, S., Schiebel, R., and Howa, H.: Population dynamics of living planktic foraminifers in the hemipelagic
1183 southeastern Bay of Biscay, *Marine Micropaleontology*, 80, 89–100,
1184 <https://doi.org/10.1016/j.marmicro.2011.06.003>, 2011.
- 1185Rigual-Hernández, A. S., Sierro, F. J., Bárcena, M. A., Flores, J. A., and Heussner, S.: Seasonal and interannual
1186 changes of planktic foraminiferal fluxes in the Gulf of Lions (NW Mediterranean) and their implications for
1187 paleoceanographic studies: Two 12-year sediment trap records, *Deep Sea Research Part I: Oceanographic*
1188 *Research Papers*, 66, 26–40, <https://doi.org/10.1016/j.dsr.2012.03.011>, 2012.
- 1189Robinson, A. R. and Golnaraghi, M.: The Physical and Dynamical Oceanography of the Mediterranean Sea, in:
1190 *Ocean Processes in Climate Dynamics: Global and Mediterranean Examples*, edited by: Malanotte-Rizzoli, P.,
1191 and Robinson, A. R., Springer Netherlands, Dordrecht, 255–306, https://doi.org/10.1007/978-94-011-0870-6_12, 1994.
- 1193Robinson, A. R., Sellschopp, J., Warn-Varnas, A., Leslie, W. G., Lozano, C. J., Haley Jr, P. J., Anderson, L. A., and
1194 Lermusiaux, P. F. J.: The Atlantic Ionian Stream, *Journal of Marine Systems*, 129–156, 1999.
- 1195Romero, O., Boeckel, B., Donner, B., Lavik, G., Fischer, G., and Wefer, G.: Seasonal productivity dynamics in the
1196 pelagic central Benguela System inferred from the flux of carbonate and silicate organisms, *Journal of Marine*
1197 *Systems*, 37, 259–278, [https://doi.org/10.1016/S0924-7963\(02\)00189-6](https://doi.org/10.1016/S0924-7963(02)00189-6), 2002.



- 1198Salmon, K. H., Anand, P., Sexton, P. F., and Conte, M.: Upper ocean mixing controls the seasonality of planktonic
1199 foraminifer fluxes and associated strength of the carbonate pump in the oligotrophic North Atlantic,
1200 *Biogeosciences*, 12, 223–235, <https://doi.org/10.5194/bg-12-223-2015>, 2015.
- 1201Schiebel, R.: Planktic foraminiferal sedimentation and the marine calcite budget: MARINE CALCITE BUDGET, *Global*
1202 *Biogeochem. Cycles*, 16, 3-1-3–21, <https://doi.org/10.1029/2001GB001459>, 2002.
- 1203Schiebel, R. and Hemleben, C.: Modern planktic foraminifera, *Paläontol. Z.*, 79, 135–148,
1204 <https://doi.org/10.1007/BF03021758>, 2005.
- 1205Schiebel, R. and Hemleben, C.: *Planktic Foraminifers in the Modern Ocean*, Springer Berlin Heidelberg, Berlin,
1206 Heidelberg, <https://doi.org/10.1007/978-3-662-50297-6>, 2017.
- 1207Schiebel, R., Waniek, J., Bork, M., and Hemleben, C.: Planktic foraminiferal production stimulated by chlorophyll
1208 redistribution and entrainment of nutrients, *Deep Sea Research Part I: Oceanographic Research Papers*, 48,
1209 721–740, [https://doi.org/10.1016/S0967-0637\(00\)00065-0](https://doi.org/10.1016/S0967-0637(00)00065-0), 2001.
- 1210Schiebel, R., Zeltner, A., Treppke, U. F., Waniek, J. J., Bollmann, J., Rixen, T., and Hemleben, C.: Distribution of
1211 diatoms, coccolithophores and planktic foraminifers along a trophic gradient during SW monsoon in the
1212 Arabian Sea, *Marine Micropaleontology*, 51, 345–371, <https://doi.org/10.1016/j.marmicro.2004.02.001>,
1213 2004.
- 1214Schmidt, D. N., Lazarus, D., Young, J. R., and Kucera, M.: Biogeography and evolution of body size in marine
1215 plankton, *Earth-Science Reviews*, 78, 239–266, <https://doi.org/10.1016/j.earscirev.2006.05.004>, 2006.
- 1216Schroeder, K., Gasparini, G. P., Borghini, M., Cerrati, G., and Delfanti, R.: Biogeochemical tracers and fluxes in the
1217 Western Mediterranean Sea, spring 2005, *Journal of Marine Systems*, 80, 8–24,
1218 <https://doi.org/10.1016/j.jmarsys.2009.08.002>, 2010.
- 1219Sen Gupta, B. K. (Ed.): *Modern foraminifera*, first published in paperback., Kluwer, Dordrecht, 371 pp., 2002.
- 1220Siccha, M. and Kucera, M.: ForCenS, a curated database of planktonic foraminifera census counts in marine surface
1221 sediment samples, *Sci Data*, 4, 170109, <https://doi.org/10.1038/sdata.2017.109>, 2017.
- 1222Siokou-Frangou, I., Christaki, U., Mazzocchi, M. G., Montresor, M., Ribera d’Alcalá, M., Vaqué, D., and Zingone, A.:
1223 Plankton in the open Mediterranean Sea: a review, *Biogeosciences*, 7, 1543–1586,
1224 <https://doi.org/10.5194/bg-7-1543-2010>, 2010.
- 1225Skinner, L. C. and McCave, I. N.: Analysis and modelling of gravity- and piston coring based on soil mechanics,
1226 *Marine Geology*, 199, 181–204, [https://doi.org/10.1016/S0025-3227\(03\)00127-0](https://doi.org/10.1016/S0025-3227(03)00127-0), 2003.
- 1227Takagi, H., Kimoto, K., Fujiki, T., Saito, H., Schmidt, C., Kucera, M., and Moriya, K.: Characterizing photosymbiosis
1228 in modern planktonic foraminifera, *Biogeosciences*, 16, 3377–3396, [https://doi.org/10.5194/bg-16-3377-](https://doi.org/10.5194/bg-16-3377-1229)
1229 2019, 2019.
- 1230Toucanne, S., Mulder, T., Schönfeld, J., Hanquiez, V., Gonthier, E., Duprat, J., Cremer, M., and Zaragosi, S.:
1231 Contourites of the Gulf of Cadiz: A high-resolution record of the paleocirculation of the Mediterranean outflow
1232 water during the last 50,000 years, *Palaeogeography, Palaeoclimatology, Palaeoecology*, 246, 354–366,
1233 <https://doi.org/10.1016/j.palaeo.2006.10.007>, 2007.
- 1234Warn-Varnas, A., Sellschopp, J., Haley, P. J., Leslie, W. G., and Lozano, C. J.: Strait of Sicily water masses, *Dynamics*
1235 *of Atmospheres and Oceans*, 29, 437–469, [https://doi.org/10.1016/S0377-0265\(99\)00014-7](https://doi.org/10.1016/S0377-0265(99)00014-7), 1999.
- 1236Wilke, I., Meggers, H., and Bickert, T.: Depth habitats and seasonal distributions of recent planktic foraminifers in
1237 the Canary Islands region (29°N) based on oxygen isotopes, *Deep Sea Research Part I: Oceanographic Research*
1238 *Papers*, 56, 89–106, <https://doi.org/10.1016/j.dsr.2008.08.001>, 2009.
- 1239Wu, H., Liu, N., Peng, J., Ge, Y., and Kong, B.: Analysis and modelling on coring process of deep-sea gravity piston
1240 corer, *J. eng.*, 2020, 900–905, <https://doi.org/10.1049/joe.2020.0077>, 2020.
- 1241Wolffteich, C. M.: *Satellite-derived sea surface temperature, mesoscale variability, and foraminiferal production in*
1242 *the North Atlantic*, M.Sc., MIT and WHOI, Cambridge, MS, 91 pp., 1994.
1243
1244
1245